Hindawi
Advances in Materials Science and Engineering
Volume 2024, Article ID 4479427, 30 pages
https://doi.org/10.1155/2024/4479427

Research Article

Design Analysis and Optimization of Coil Spring for Three-Wheeler Vehicles Using Composite Materials

Solomon Nigusu Abera[1] **and Bisrat Yoseph Gebreyesus**[2]

[1]*Department of Automotive Engineering, Faculty of Mechanical and Industrial Engineering, Bahir-Dar Institute of Technology, Bahir-Dar University, Bahir-Dar, Ethiopia*
[2]*Motor Vehicle Engineering Department, College of Engineering, Defence University, P.O. Box 1041, Bishoftu, Ethiopia*

Correspondence should be addressed to Solomon Nigusu Abera; solomon.nigusu@aastustudent.edu.et

Received 16 February 2023; Revised 9 December 2023; Accepted 19 December 2023; Published 6 January 2024

Academic Editor: Dimitrios E. Manolakos

The quest for lightweight, efficient, and corrosion-resistant coil springs for vehicle suspension systems has led to the exploration of alternative materials beyond traditional steel. This study delves into the potential of composite materials, particularly carbon/epoxy and carbon/carbon nanotube/epoxy, as replacements for conventional steel coil springs in light vehicles. Through a comprehensive analysis of mechanical properties under static and dynamic loading conditions, the study demonstrates the superior performance of composite springs compared to their steel counterparts. After optimization, the deflection of the carbon/carbon nanotube/epoxy and carbon/epoxy springs decreased to 15.003 mm and 18.703 mm, respectively, and the maximum shear stress decreased by 64.63% and 62.2%, respectively. Likewise, strain energies increased to 2.3644 and 3.5616, respectively. The springs were also studied under dynamic conditions, and the result showed these springs have the ability to perform in dynamic conditions. The carbon/carbon nanotube/epoxy composite emerged as the frontrunner, exhibiting remarkable improvements in shear stress, fatigue life, strain energy, and deformation properties. The study highlights the ability of carbon/carbon nanotube/epoxy composite springs to significantly reduce weight, enhance efficiency, and extend fatigue life, making them a promising alternative for next-generation vehicle suspension systems.

1. Introduction

Of the most significant systems that vehicles have, the suspension system is the first one to play a significant role in the passenger's safety and comfort. It dissipates kinetic energy to regulate shocks and vibrations caused by the road surface so that passengers and the vehicle structure are not harmed or disturbed. The suspension system includes all of the components that connect the tires to the vehicle body as shown in Figure 1. In most automobile vehicles, shock absorbers and springs are used to decrease the influence of traveling over the harsh road, which leads to improved vehicle control and quality of the ride [2–4].

Springs are elastic bodies that deform when loaded and later return to their original shape when the force is withdrawn. In most new passenger cars, light coil springs are now standard. Most commercial cars have a coil spring in the front and a leaf spring in the back. A coil spring is constructed from a certain wire that has been heat-treated to give it the spring shape that is needed. The shape (kind of spring), the overall diameter of the spring, and wire diameter, all influence the spring's load-bearing capacity. Excessive cyclic fatigue, as well as poor quality spring materials, could lead to the spring's failure. Most of the time, highly used springs are made of hardened steel. Small size springs can be constructed from prehardened steel, while larger ones are made from annealed steel and then hardened after fabrication [5].

The springs used on vehicles' suspension systems have been studied by different scholars from different perspectives. Conservation of resources and economic energy

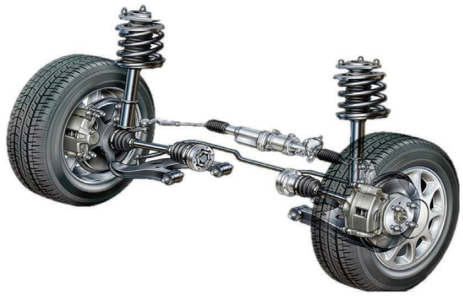

Figure 1: Vehicle suspension system components [1].

usage is now a hot research area for scholars and automobile manufacturing companies. Some of the primary methods used by researchers to reduce the weight of an object are design optimization, selection of advanced materials, and using efficient manufacturing processes. A coil spring is one of the essential components in light vehicles that can affect the unsprung weight of the suspension system as well as the overall weight of the vehicle. Fuel efficiency and improved ride quality are advantages that can be achieved by minimizing the weight of components in the system of a vehicle. Using composite materials, the coil springs of light vehicles have been made lighter than steel springs without sacrificing load-carrying capacity or stiffness. This is because composite materials have a higher strength-to-weight ratio than steel materials, which means they can store more elastic strain energy.

The whole suspension system protects the vehicle body from road shocks and vibrations, which would otherwise be transmitted to the passengers and cargo. Regardless of the road surface, it must maintain the tires in contact with the road. Solid or beam axles join either side of the vehicle wheel. With independent suspension, the movement of one wheel on the one side of the vehicle is communicated to the opposite wheel, allowing the wheels to move independently of one another and reducing body movement. It also lowers body movement by preventing the opposite wheel from being impacted by the opposite wheel's movement. The front suspension of most current light vehicles is made out of coil springs as it is shown in Figure 2. Then, the spring acts as an elastic object used to store mechanical energy. It can be twisted, pulled, (or) stretched by some force and can return to its original shape when the force is released.

A coil spring is formed from a single length of a special wire that is heated and wound on a former to give it the shape it needs. Small size springs can be constructed from prehardened steel, while larger ones are made from annealed steel and then hardened after fabrication [5]. The diameter of the wire, the total diameter of the spring, its shape, and the spacing of the coils are some of the parameters that could affect the spring's load-carrying capacity and performance. Most failures of existing coil spring are due to high cyclic fatigue and poor material properties. For example Pictures of failed coil springs are given in Figure 3.

1.1. Composite Materials. The first recorded composite, wattle and daub, was used to construct walls over 6,000 years ago, even if it was eventually supplanted by various types of composites [8]. Although composites are generally constructed of manmade components, natural materials such as wood also exist. Many studies have shown that the composite's properties are improved over its constituents' properties. A composite is comprised of two phases, which are reinforcement and matrix. The matrix part includes the reinforcing phase, which is responsible for the matrix's strength [9–11]. These two components have their own characteristics, and when combined, they will determine other different properties and behaviors of the overall composite material [12]. Composite materials refer to materials in which two or more distinct materials are combined together but remain uniquely identifiable in the mixture, having strong fibers surrounded by a weaker matrix material. The matrix serves to distribute the fibers and also transmit the load to the fibers. The mechanical and structural integrity of a structural composite is determined by the qualities of each constituent's specific compositions as well as the geometrical designs of the bulkier structural parts, such as shape and size [13].

Fiber-reinforced polymer composite (FRP) is a broadly known type. Even if there are many kinds of FRP, the two most familiar ones are carbon fiber-reinforced composite (CFRC) and glass-reinforced plastic (GRP). As their name indicates, the fiber materials used for CFRC and GRP are carbon and glass, respectively, and the matrix, also known as a binder, is an epoxy resin, which is a thermoplastic material. There are also other types of composites, including wood composites, polymer matrix composites (PMC), metal matrix composites (MMC), ceramic matrix composites (CMC), and the materials known as advanced composites (ACM). The incorporated materials in PMC, MMC, and CMC are polymeric, metallic, and ceramic materials, respectively, and these composites are collectively called conventional composites [11, 14]. Since ACMs are fabricated using high-strength, low-density fibers, they have a higher modulus of elasticity, stiffness, and strength and lower densities than conventional composites. These composite materials also have important properties such as ease of manufacture and resistance to chemicals, temperature, and creep [15].

Generally, composite materials can be used in a variety of applications in society. Some of these applications include uses in the construction industry as a building material, the automotive industry for automobile parts such as bodies, aeronautics, where materials with high strength and low density are required, the manufacture of housing and industrial parts such as shower stalls, washing sinks, storage tanks, and bathtubs, and the medical world as biomaterials for tissue replacements and regenerative medicine [9, 16–18]. As it is stated by many scholars in this study area, highly accurate and specific material properties can be manufactured with the simplest of manipulations of some parameters, such as the constituents' volume ratios, fiber particle size, geometry, orientation and distribution, and matrix type. This makes composite materials more flexible

Figure 2: Coil spring installed on front suspension of three-wheeler vehicles.

Figure 3: Failure of helical vehicle coil springs [6, 7].

for design and can easily be customized to have almost any desired property combination, unlike metallic, polymeric, and ceramic biomaterials [19, 20].

1.2. Properties of Composites. It is previously mentioned that the unique flexibility behavior of composites in their design and manufacture enables them to exist in various property combinations. Therefore, unlike traditional materials, for example, steel, there are no fixed values for the properties of composites. However, one characteristic property that is common with almost all composite materials is their low weight-to-strength ratio. This behavior makes them widely applicable in many industries such as automobile, biomedical, and aerospace industries [21, 22]. Composites are typically designed ahead of other materials to have the specified load-carrying capability and other performance features. Low weight-to-strength ratio, high fatigue resistance, high corrosion resistance, creep resistance, low thermal and electrical conductivity, high wear resistance, and high impact strength are some of the advantages that can be gained from composite material products [19, 23].

1.2.1. Nanocomposites. A nanocomposite, according to Twardowski [24], is a composite material in which one of the components has at least one nanoscopic dimension of roughly 10^{-9} m. To achieve uniform dispersion of nanofillers in the holding matrix using various approaches, researchers are investigating feasible alternates. Due to their superior consistency and structural, electrical, and mechanical properties, polymer nanocomposites have shown significant potential as a future material in a variety of technical applications [25–29]. A polymeric material (e.g., elastomers, thermosets, or thermoplastics) is combined with a reinforcing nanoscale substance to form polymer nanocomposites (PNs) (nanoparticles). Mechanical qualities, gas barrier properties, thermal stability, fire retardancy, and other features of polymer nanocomposites have all improved dramatically. When nanoparticles are integrated into a polymer matrix, there are various advantages such as mechanical properties (tensile strength, stiffness, and toughness) and dimensional stability.

1.2.2. Carbon Nanotubes. From the nanoparticle materials, carbon nanotube (CNT) was selected for this research work. Carbon nanotubes have attracted much attention in the past several years because of their unique potential uses for structural, electrical, and mechanical properties. Nanotubes have a high Young's modulus and tensile strength, and they can be metallic, semiconducting, or semimetallic, depending on the helicity and diameter [28]. Carbon nanotubes are excellent candidates for stiff and robust structures because the carbon-carbon bond in graphite is one of the strongest in nature. Transmission electron microscopy data revealed that carbon nanotubes are flexible and do not break upon bending [28, 30]. The thermal conductivity of carbon nanotubes can be extremely high, and the thermal conductivity of individual carbon nanotubes was found to be much higher than that of graphite and bulk nanotubes [31]. They have a wide spectrum of potential applications.

Examples include use in catalysis, storage of hydrogen and other gases, biological cell electrodes, quantum resistors, nanoscale electronic and mechanical devices, electron field emission tips, scanning probe tips, flow sensors, and nanocomposites. Carbon nanotubes can be grouped as single-wall (SWCNT), multiwall (MWCNT), and the newly established small-diameter (SDCNT) material, based on the number of walls present in the carbon nanotubes, as illustrated in Figure 4 [29].

MWCNTs are multiwalled carbon nanotubes with inner diameters ranging from 2 to 10 nm, outer diameters ranging from 20 to 70 nm, and lengths of about 50 μm, while SDCNTs have diameters of less than 3.5 nm and lengths ranging from several hundred nanometers to several micrometers. These SDCNTs generally have one to three walls [32]. According to the researchers' papers, the density of single-walled carbon nanotubes (SWCNT) is less than one-sixth of that of steel, while the density of multiwalled carbon nanotubes (MWCNT) is one-half of that of aluminum. The tensile strengths of SWCNTs and MWCNTs are known to be in a range much greater than that of high-strength steel, and their Young's modulus values are almost similar to that of a diamond. They are highly resilient in that they can assist with large angle bending and recover with no damage, which makes them different from the metal's plastic deformation and the carbon fiber's brittle fracturing. Likewise, theoretically, their electrical and thermal conductivities are comparable to diamonds', with an almost negligible thermal expansion coefficient. These materials also have high thermal stability in the air as well as in a vacuum, when compared with the lower values of metal wires in microchips [33, 34].

The aim of this paper is to design composite materials in such a way that they could replace the steel material used for helical coil spring construction while maintaining all performance standards. The composite materials whose properties are in advance for the desired function are selected according to the reviewed literature papers and the mechanical properties of these composites are designed carefully to fit the coil spring parameters.

2. Literature Review

There are many researchers who investigated advanced materials to be used for coil springs beyond the conventional steel material which is mostly used in the coil spring manufacturing world. This has been discussed by a great number of authors in literature. Those researchers proved that the conventional steel material can be replaced by other new materials, or that could have some additional importance in being used as a material for coil springs and could improve the efficiency of the spring as well as the vehicle. The choice of composite materials significantly impacts spring performance. Recent studies have explored diverse fiber reinforcements, including carbon fiber, glass fiber, aramid fiber, and natural fibers such as bamboo and flax. Researchers emphasize the importance of considering fiber orientation and laminate configuration to optimize stiffness, strength, and fatigue resistance [5, 35–37]. Several optimization techniques are employed to achieve desired spring

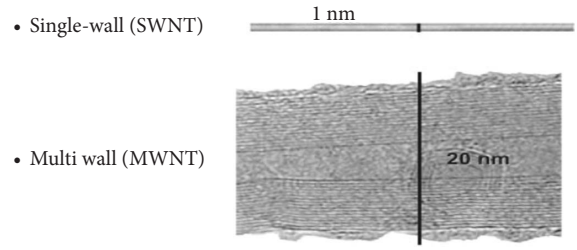

Figure 4: Definition of single- and multiwall carbon nanotubes [32].

performance. Finite element analysis (FEA) is prominently used to predict spring behavior under various loading conditions and identify areas for improvement. Optimization algorithms such as genetic algorithms, particle swarm optimization, and artificial neural networks are employed to optimize design parameters such as fiber volume fraction, fiber orientation, and geometric dimensions. Additionally, topology optimization techniques are gaining traction, allowing for the creation of novel spring designs with improved efficiency. Accurately analyzing and modeling the behavior of composite coil springs is crucial for a reliable design. Researchers are actively developing advanced computational models that incorporate material nonlinearities, anisotropic properties, and contact mechanics. These models are validated through experimental testing, ensuring accuracy and reliability [9, 20, 22, 38–47].

A study by Gaikwad and Kachare [5], using the NASTRAN solver, examined the static analysis of the helical compression spring used in the two-wheeler horn and compared it with analytical results. Static analysis determines the safe stress and corresponding payload of the helical compression spring. Another researcher Singh Pankaj et al. [48] has researched about the materials used for unicorn bike's monoshock suspension spring production. For diverse spring materials and changing wire diameters of springs, the statistical structural analysis is done using the FEA method in ANSYS. Materials such as 1095, 5160 carbon steel, cobalt chrome, chrome vanadium, and beryllium copper are used. The car is assumed to be moving for these calculations. The authors compared the final results and selected the best among them. A similar methodology is also followed by Kumar et al. [49] to replace the existing chrome vanadium material by 60Si2MnA steel after comparing the deflection and stress properties. The weight of a vehicle was successfully lowered by substituting steel with composite materials in another study by Choi and Choi [50], by considering optimization of the material characteristics and design factors of the structure through numerical and experimental methods to calculate the ply angles and wire diameters of carbon fiber/epoxy composite coil springs to achieve a spring rate comparable to that of a steel component. In the study, the shear modulus ratio was computed as a function of the ply angles; normalized spring rates for certain ply angles and wire diameters were computed and compared. In another study [51], three distinct composite helical springs have been used to replace steel helical springs: glass/epoxy, carbon/epoxy, and Kevlar/epoxy. The

properties of composite springs have been investigated by varying the fiber angle relative to the spring axis. The study shows that shear stress decreases as the fiber angle changes, and it reaches its lowest value when the fiber's position is perpendicular to the load [52]. Similarly, Budan and Manjunatha [53] investigated that the conventional steel coil spring can be replaced by a composite coil spring to reduce the weight. The study uses three springs of glass fiber, carbon fiber, and a combination of glass fiber and carbon fiber. The laboratory experiments exhibited that the spring rate of the carbon fiber spring is higher than that of other springs. The three composite springs are lighter in their weight and have less stiffness value than that of conventional steel springs. Carbon fiber springs have a higher stiffness than the other two forms of composite coil springs. Finally, the researcher concluded that steel springs can be replaced by high-strength carbon fiber springs.

Some other scholars also studied RUC-based multiscale models for braided reinforced polymers for coil spring application. The researchers used a multiscale approach (yarn scale, braid scale, and component scale), comprising three scales of observation. The simulation findings demonstrate a high level of agreement with experimental observations and provide insights into the stress distribution within the coil as well as the sensitivity of design parameters to spring performance [54]. Similarly, the use of composites for spring construction has been also mentioned in the research by Suresh and Thiagararajan, which is the design and experimental analysis of a composite helical spring made of a fiber-reinforced polymer of woven roving fiber (WRF) and thermoset polymer (epoxy resin) with nanoclay. The goal was to see how a composite helical spring compared to a steel helical spring in terms of load-carrying capacity, stiffness, and weight savings [55].

A research paper by Prawoto, Ikeda, Manville, and Nishikawa discusses coil springs used in automotive suspension and studies their fundamental stress distribution, manufacturing process, common failures, and material characteristics. This paper also discusses several case studies of suspension spring failures, and the presented failures range from the very basic to failures due to complex stress usage and chemically induced failures. The study also presents a FEA of stress distributions on typical failure initiation sites [56, 57]. Another methodology is also used by Shevale and Khaire [58], which focuses on the fatigue stress analysis and fatigue life of springs used in Maruti-Suzuki Alto K10. The study employs experimentation using a strain gauge with the help of the Wheatstone network to validate the results. Yogesh Chaubey [59] conducted research on the failure analysis of suspension coil springs, with the goal of analyzing failure in vehicle coil springs. According to the authors' work, failure of a spring is caused by fatigue analysis, a surface imperfection in a coil spring, internal faults in a coil spring, corrosion in a coil spring, and other factors. It appears that the suspension system's materials have flaws that are causing them to fail prematurely. The research by Christopher, Pavendhan [60], and Logavigneshwaran et al. [61] focused on designing and examining the performance of the motorcycle coil spring shock absorber by changing the spring diameter. Pro/ENGINEER and ANSYS software are used in both studies. The diameter of the shock absorber is reduced, which improves the design. Pastorcic et al. [62] investigated the failure and fatigue analysis results of a coil spring that had failed in service. The authors examined the failed coil spring and determined the causes of the fracture. Through the quarter-car model for dynamic loading conditions, MATLAB numerical routine and Miner's cumulative damage assessment in keeping with the Goodman failure criterion, the results gave a good prediction about the spring's fatigue life.

Generally, the literature papers above mention that the spring design is critical in terms of strength and durability and the reduction of spring weight is also a key factor in improving automotive dynamics. The use of a composite helical spring instead of a steel helical spring reduces spring weight while also increasing resistance to applied stress. In this research paper, composite materials are selected to replace the existing conventional steel by comparison. The two major composites to be used for coil spring applications are carbon/epoxy (single fiber and single matrix composite) and carbon/carbon nanotube/epoxy (two fibers and single matrix composite). Static and dynamic analyses are used in this study to analyze the behavior of steel and composite helical springs in light car suspension systems. A steel spring was substituted by two different composite springs, and the load-carrying capacity, stiffness, and weight savings (strength-to-weight ratio) of the composite helical spring are compared with those of a steel helical spring. The material selection is based on their advanced properties for the application of compression coil springs. The study also considers many previously published research papers to select the most advanced composites for coil spring applications [38, 39, 50, 52, 55, 63–66].

3. Methodology

3.1. Composite Materials and Design Methodology

3.1.1. Fiber Selection. Fibers are the principal constituents of fiber-reinforced composite materials and bear the majority of the load acting on them; fiber type, fiber volume fraction, fiber length, and fiber orientation are all important factors to consider throughout the composite design process. According to Mallick [67], four fiber characteristics have a significant impact on the mechanical performance of a composite material (length, orientation, shape, and material). Therefore, in this study, all these characteristics are considered during fiber selection (Figure 5).

(1) Carbon Fiber. Carbon fibers are a new generation of high-strength materials composed of graphitic and noncrystalline regions. Carbon fibers have the strongest specific modulus and strength of all reinforcing fibers. They may also maintain their tensile strength even at high temperatures and are moisture-resistant. In contrast to glass and other organic polymer fibers, carbon fibers do not necessarily break when stressed. They are extremely versatile because of their outstanding strength-to-weight and stiffness-to-weight ratios

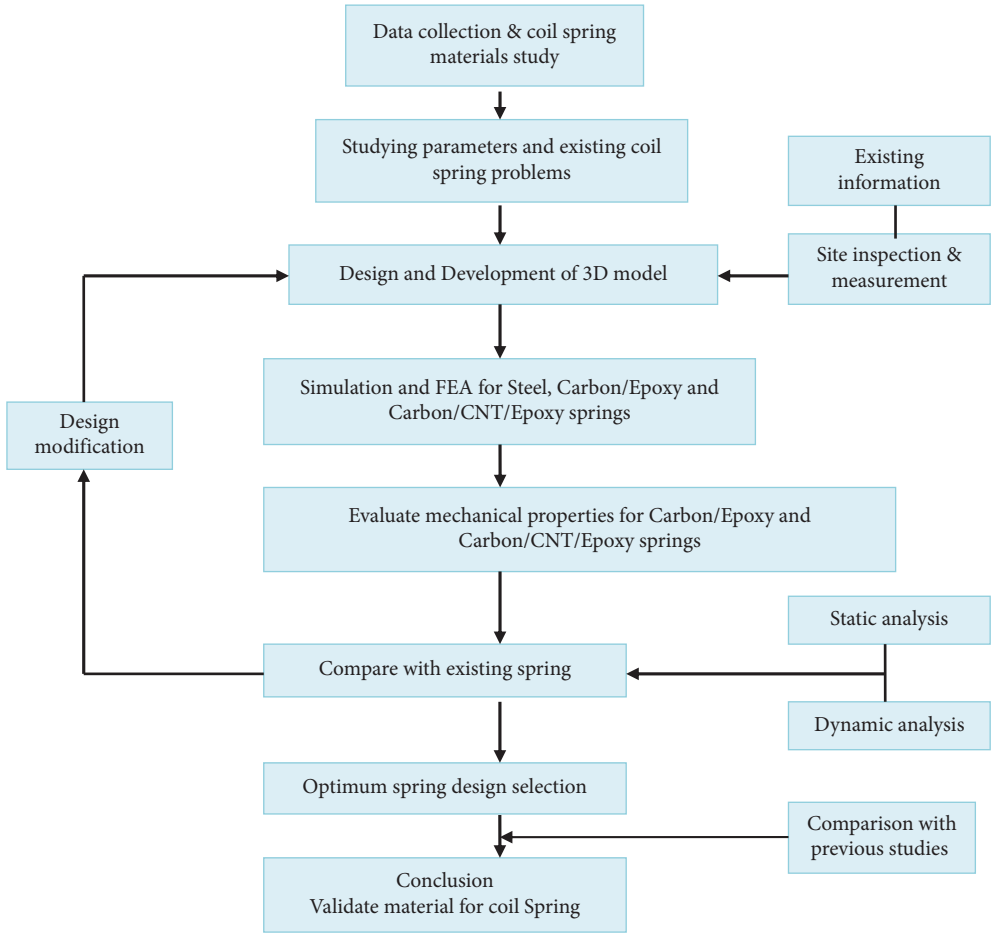

Figure 5: Methodology.

which are stiffness and modulus of elasticity that range from glass to three times that of steel. They are also chemically inert, electrically conductive, and incombustible [68].

(2) Carbon Nanotube (CNT). Carbon nanotubes are unique tubular structures of nanometer diameter and large length to diameter ratio. Carbon nanotubes (CNTs) are allotropes of carbon with a nanostructure that can have a length-to-diameter ratio greater than 1,000,000. The nanotubes may consist of one up to tens and hundreds of concentric shells of carbons with adjacent shells separation of approximately 0.34 nm. Nanotubes are long, thin cylinders of carbon; they are 100 times stronger than steel, very flexible, and have unique electrical properties. Their electrical properties change with diameter, "twist," and number of walls. Carbon nanotubes can be either conducting or semiconducting in their electrical behavior. Due to their exceptional mechanical, thermal, and electrical properties, in addition to low density with respect to the class of organic and inorganic tubes, carbon nanotubes (CNTs) are extremely promising for the development of high-performance nanostructured materials [25, 27–30, 69–71]. They are broadly classified as single-walled carbon nanotubes and multiwalled carbon nanotubes. According to Eatemadi and his colleagues, the general differences between single-walled carbon nanotubes/SWCNTs and multiwalled carbon nanotubes/MWCNTs are summarized in Table 1 [64].

3.1.2. Resin Selection. The matrix binds the fiber reinforcement, transfers load between fibers, gives the composite component its net shape, and determines its surface quality. A composite matrix may be a polymer, ceramic, metal, or carbon [72–74]. Although matrices by themselves generally have low mechanical properties compared to those of fibers, they can still influence many mechanical properties of the composites such as transverse modulus and strength, shear modulus and strength, compressive strength, inter laminar shear strength, thermal expansion coefficient, thermal resistance, and fatigue strength.

(1) Epoxy Resins. Composite fibers are nothing without introducing epoxy. Although reinforcing fibers are used in many applications, epoxy is the substrate that we will be dealing with. The substrate materials are used to bind whatever strengthening fiber is being used and to lock them in position so they can stay in position to do their job. Then, for these composite fibers, epoxy is as a substrate material. Epoxy is a thermosetting polymer with varied qualities including mechanical conductivity, thermal conductivity,

Table 1: Comparison between single-walled and multiwalled carbon nanotubes [64].

Single-walled carbon nanotube/SWCNT	Multiwalled carbon nanotube/MWCNT
(i) Single layer of graphene	(i) Multiple layers of graphene
(ii) Catalyst is required for synthesis	(ii) Can be produced without a catalyst
(iii) Bulk synthesis is difficult	(iii) Bulk synthesis is easy
(iv) Proper control over growth and atmospheric condition	
(v) Purity is poor	(iv) Purity is high
(vi) A chance of defect is more during functionalization	(v) A chance of defect is less, but once occurred, it is difficult to improve
(vii) Less accumulation in the body	(vi) More accumulation in the body
(viii) Characterization and evaluation are easy	(vii) It has a very complex structure
(ix) It can be easily twisted and is more pliable	(viii) It cannot be easily twisted and is more pliable

and low density, but high brittleness. It can be used as a matrix, adhesive, and coating. Many researchers work to make the epoxy-based material less brittle in order to increase its ductility [71, 75]. Epoxy-based nanocomposites have several uses in the automotive, airplanes, sports equipment, marine, and biomedical industries [25, 41, 76].

In general, epoxy resins have very good adhesive properties, superior mechanical properties, i.e., strength and stiffness, better resistance to fatigue and micro-cracking, high resistance to water penetration, faster curing at room temperature, and good chemical resistance properties [77].

Other than the fiber and the matrix, there are also factors that influence the mechanical performance of a composite such as the fiber-matrix interface. It determines how well the matrix transfers the load to the fibers. Chemical, mechanical, and reaction bonding may form the interface. Based on the design and required operating environments, any material can be used to manufacture a spring, as long as the materials have the required combination of rigidity and elasticity. At this time, the automobile industries are regularly trying to lessen the fuel consumption of the automobile vehicles and working on the maximization of fuel efficiency of automobiles in different ways, especially by lowering the weight of the vehicle. Currently, the need for a material with light weight and high performance is increasing day by day. Improvement of the performance for a material is limited when there is only one composition. Therefore, there should be a new material with high performance which constitutes two or more conventional materials [78, 79].

In this research paper, composite materials are selected to replace the existing conventional steel by comparison. The two major composites to be used for coil spring applications are carbon/epoxy (single fiber and single matrix composite) and carbon/carbon-nanotube/epoxy (two fibers and single matrix composite). The selection of these composites is based on their advanced properties for the application of compression coil springs. The study also considers many previously published research papers to select the most advanced composites for coil spring application [35–37, 41, 46, 50, 52, 55, 63–65, 71, 78, 80].

(2) Micromechanics. The Rule of mixtures method provides approximate upper- and lower-bound estimates for composite material parameters such as elastic modulus, mass density, ultimate tensile strength, thermal conductivity, and electrical conductivity [81]. This approach involves some assumptions. The first is about the matrix, which is assumed to be free of voids and to have a perfect bond with the fiber. Uniform distribution of the fiber throughout the matrix is also assumed. Some additional assumptions are that the lamina is initially free from any residual stresses. The fiber and the matrix are taken as linearly elastic materials. Also, the applied loads are either parallel or normal to the fiber direction.

4. Composite Materials' Mechanical Property Determination

4.1. Weight Fraction and Volume Fraction. Most micromechanics-based techniques use mass and volume fractions, along with specific phase properties, to represent the properties of the comparable homogeneous material. In the present case, the effective properties of a composite are obtained with the assumption that the fiber is orthotropic or transversely isotropic and that the matrix is isotropic in behavior. However, with appropriate changes, fiber can also be considered isotropic. The subscripts or superscripts (f) and (m) in the next description denote fiber and matrix, respectively. The general formulas for weight fraction and volume fraction for fiber and matrix are described below.

4.1.1. Weight Fraction. Let w_f, w_m, and w_m be the weight of fibers, matrix, and composite, respectively. The weight fractions are defined as the ratio of the weight of the respective phase to the mass of the composite.

(1) Weight fraction of the fiber (W_f): [82].

$$W_f = \frac{\text{weight of fiber}}{\text{total weight}} = \frac{w_f}{w_t} = \frac{w_f}{w_m + w_f}. \quad (1)$$

(2) Weight fraction of matrix (W_m): [82].

$$W_m = \frac{weight\ of\ matrix}{total\ weight} = \frac{w_m}{w_t} = \frac{w_f}{w_m + w_f}, \quad W_f + W_m = W_c = 1. \tag{2}$$

The fiber volume fraction (V_f) is defined as the ratio of fiber volume (v_f) to composite volume (v_c), and matrix volume fraction (V_m) is defined as the ratio of matrix volume (v_m) to composite volume.

(3) Volume fraction of the fiber (V_f):

$$V_f = \frac{v_f}{v_c} = \frac{\text{volume of fiber component}}{\text{volume of composite}}. \tag{3}$$

(4) Volume fraction of the matrix (V_m):

$$V_m = \frac{v_m}{v_c} = \frac{\text{volume of matrix component}}{\text{volume of composite}}. \tag{4}$$

The volume fractions of a matrix and fiber added together must be equal to one.

For a carbon/epoxy composite, which has a two-component system consisting of one fiber and one matrix, the total volume fraction of the composite is calculated as follows:

$$V_c = V_m + V_f = 1, \quad \text{hence} = V_m = 1 - V_f. \tag{5}$$

4.1.2. Density of the Composite. By considering the weight of composite w_c is the sum of the weight of the fibers w_f and the weight of the matrix w_m, the density of the composite can also be derived in terms of volume fractions.

$$W_f + W_m = W_c. \tag{6}$$

The weights can be expressed in terms of their respective densities and volumes [65] as follows:

$$\rho_c v_c = \rho_f v_f + \rho_m v_m, \quad \rho_c = \rho_f V_f + \rho_m V_m. \tag{7}$$

Therefore, the calculated values for the densities of the two composites will be listed below for different proportions of matrix and fiber. Then, the better proportion of matrix to fiber will be selected for a coil spring material (Table 2).

Many scholars in the literature stated that the volume fraction of fiber to the matrix of 60/40 has better advantages in terms of the chemical and physical properties of the composites. Due to their remarkable mechanical qualities and low density, carbon nanotubes (CNTs) have found a novel application as a reinforcing nanofiller in composite materials [42, 71, 83, 84]. Multiscale composites' tensile, shear, and flexural properties are increased by CNTs' high strength and stiffness [85]. The fact that even small levels (5 wt%) of CNT loading result in appreciable changes in their mechanical and physical properties is evidence of the efficacy of CNT reinforcing [71]. The creation of high-performance CNT/polymer composites with CNT contents between 0.1 and 5 wt% has been the subject of numerous investigations [86, 87]. According to literature reviews, a composite composition with 60% fiber offers good qualities. Therefore, 60% of the volume of carbon fiber is made up of carbon fibers in the composite material carbon/epoxy, 1% of the volume is made up of carbon nanotube fibers, and 59% of the remaining 40% is matrix (epoxy resin).

So, as it is stated in the above table and information from literature reviews, volume fraction of fiber = 0.6, volume fraction of matrix material (epoxy) = 0.4, density of carbon fiber = 1.75 g/cm^3, and density of epoxy = 1.2 g/cm^3. Based on the above formulas, the density of composite carbon/epoxy material (ρ_c) will be

$$\rho_c = \frac{1.53g}{\text{cm}^3}. \tag{8}$$

Longitudinal and transverse properties of the composite material (P_c) are estimated as follows:

$$P_c = P_f V_f = P_m V_m, \tag{9}$$

where P_f and P_m are material properties of fiber and matrix, respectively.

According to Buragohain [88], this equation can be easily explained using stiffness calculation analogy for two parallelly connected springs as it is given in Figure 6.

For properties perpendicular to fiber direction, the calculation becomes a little more sophisticated, dependent on the fiber shape and fiber content, but a good estimate can be obtained using the model of two springs connected in series as shown in Figure 7:

With this model, the total deformation at a point of load application in a direction perpendicular to fiber direction is the sum of the deflections in the fiber and the matrix. The

Table 2: Fiber percentage effects in mass of composite materials.

Weight of springs (kg)	Fiber percentage of the composite springs			
	50%	60%	70%	80%
Conventional steel spring	2.02	2.02	2.02	2.02
Carbon/CNT/epoxy composite spring mass (kg)	0.379	0.393	0.407	0.422
Carbon/epoxy composite density	1.475	1.53	1.583	1.64

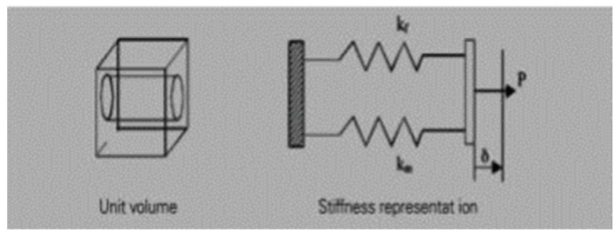

Figure 6: Physical model for the longitudinal properties of a composite [88].

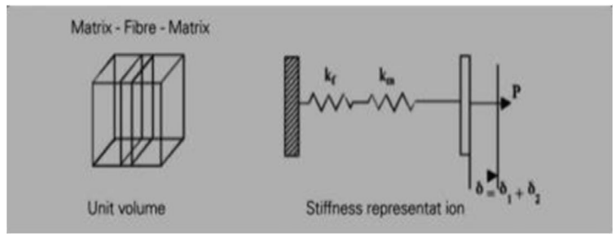

Figure 7: Physical model for the transverse properties of a composite [88].

resulting expression for transverse property of a composite is as follows:

$$\frac{1}{P_c} = \frac{V_f}{P_f} + \frac{V_m}{P_m}. \tag{10}$$

4.2. Mixture Rule. Using the formulas in Table 3 and some assumptions, the longitudinal mechanical properties of carbon/epoxy composite are determined. According to Buragohain [88], we use stiffness calculation analogy for two parallelly connected springs. The properties of the carbon/CNT/epoxy are also determined using similar methodologies. The transverse properties for both composite types are also determined using the mixture rule approach integrated with the Hooks law (Table 3).

The following assumptions are taken in this method:

(1) Perfect contact exists between the fibers and the matrix. This assumption leads to the following equality.

(2) Additional stresses that are perpendicular to direction of the fiber placement are negligible (in a general case, these stresses are due to different values of the Poisson coefficients of the fiber and the matrix).

(3) Total transverse deformation is the sum of deformation of the fiber and the matrix multiplied by their volume fractions:

To find longitudinal Young's modulus E_1 and Poisson's ratio μ_{12}, the loading along the direction of the fibers will be considered as shown in Figure 8 [89].

The force acting on the cross-section of the composite is the sum of the forces acting on the fiber and the matrix. Using the above equations, the following expressions effective Young's modulus E_1 and Poisson's ratio μ_{12} can be obtained.

The characteristics of the composite in the direction normal to, rather than parallel to, the fibers are referred to as transverse properties, as is shown in Figure 9.

To determine the effective Young's modulus E_2 and Poisson's ratio μ_{23}, the scheme of loading transversely to the direction of the fiber placement is used as shown in Figure 10. [89]

Then, the shear modulus G_{12} can also be calculated according to shear deformation for composite materials as shown in Figure 11.

Assuming that the total stress and stress of the matrix and fiber are equal to each other,

$$\begin{aligned} \sigma_{12} &= \sigma_{12}^{f} \\ &= \sigma_{12}^{m}. \end{aligned} \tag{11}$$

As it is indicated in the figure,

$$\Delta = \Delta_m + \Delta_f. \tag{12}$$

From the three equations given above, the effective shear modulus can be given as follows:

Table 3: The general formulas used in the determination of mechanical properties.

Assumptions	General formulas	
$\varepsilon_{11} = \varepsilon_{11}^{f} = \varepsilon_{11}^{m}$	$W_f = w_f/w_t = w_f/w_m + w_f$	$\rho_c v_c = \rho_f v_f + \rho_m v_m$ $\rho_c = \rho_f V_f + \rho_m V_m$
$\varepsilon_{22} = V_f \times \varepsilon_{22}^{f} + V_m \times \varepsilon_{22}^{m}$	$W_m = w_m/w_t = w_f/w_m + w_f$	$P_c = P_f V_f = P_m V_m 1/P_c = V_f/P_f + V_m/P_m$ (transverse)
$\varepsilon_{22} = V_f \times \varepsilon_{22}^{f} + V_m \times \varepsilon_{22}^{m}$	$V_f = v_f/v_c, V_m = v_m/v_c V_c = V_m + V_f$	Hooks law $\varepsilon_{11} = \sigma_{11}/E_1 \quad \varepsilon_{11}^{f} = \sigma_{11}^{f}/E_1 \quad \varepsilon_{11}^{m} = \sigma_{11}^{m}/E_m\, \varepsilon_{22} = -\mu_{12}\varepsilon_{11} \quad \varepsilon_{22}^{f} = -\mu_{12}^{f}\varepsilon_{11}^{f} \quad \varepsilon_{22}^{m} = -\mu_{12}^{m}\varepsilon_{11}^{m}$
$\sigma_{11} = \sigma_{11}^{f} V_f + \sigma_{11}^{m} V_m \sigma_{22} = \sigma_{22}^{f} = \sigma_{22}^{m} \sigma_{22} \neq 0, \sigma_{11} = \sigma_{33} = \sigma_{12} = \sigma_{23} = \sigma_{31} = 0$	$E_1 = V_f \times E_1^{f} + V_m \times E_1^{m}\, \mu_{12} = V_f \times \mu_{12}^{f} + V_m \times \mu_{12}^{m}$	$E_2 = (E_2^{f} E_2^{m})/(V_f E_2^{m} + V_m E_2^{f})\, \mu_{12} = (\mu_{23}^{f} \mu_{23}^{m})/(V_f \mu_{23}^{m} + V_m \mu_{23}^{f})$ $\varepsilon_{12} = G_{12}/G_{12}, \varepsilon_{12}^{f} = G_{12}^{f}/G_{12}^{f}, \varepsilon_{12}^{m} = G_{12}^{m}/G_{12}^{m}$

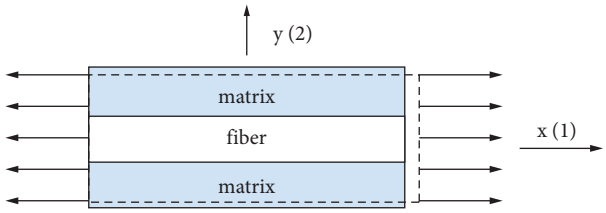

Figure 8: The loading of the sample along the fiber direction [89].

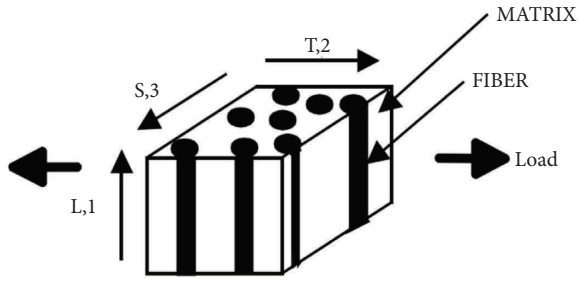

Figure 9: Transverse loading of a composite.

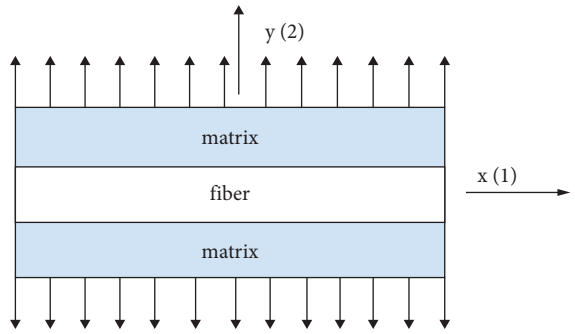

Figure 10: The loading of the sample across the fiber packing [89].

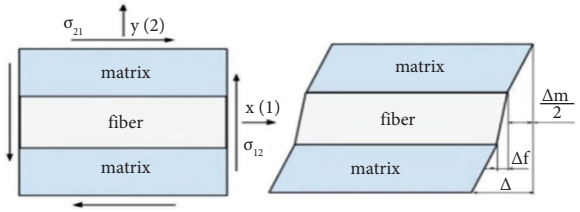

Figure 11: Shear deformation of the composite material [89].

$$G_{12} = \frac{G_m.G_f}{G_m.V_f + G_f.V_m}. \tag{13}$$

Longitudinal modulus (E_1) for carbon/epoxy composite: Equal strain assumption:

$$\begin{aligned} \varepsilon_c &= \varepsilon_m \\ &= \varepsilon_f. \end{aligned} \tag{14}$$

The load, however, is partitioned between the fiber and the matrix as follows:

$$P_c = P_f + P_m. \tag{15}$$

Static equilibrium states that the elemental total resultant force must be equal with the sum of the forces acting on the fiber and matrix. σ_f and σ_m are the stresses on the fiber and matrix, respectively.

If the length of composite is assumed to be 1, then the areas A_m, A_f and A_c can be considered volumes V_m, V_f and V_c.

Strain compatibility is determined by equating the average strains in the composite fiber and matrix along their longitudinal axes. Therefore,

$$\begin{aligned} E_1 &= E_f \times V_f + E_m \times V_m = 230 \times 0.6 + 3.45 \times 0.4, \\ E_1 &= 139.38. \end{aligned} \tag{16}$$

All the required mechanical properties of both carbon/epoxy and carbon/CNT/epoxy composites are calculated using the proper mixture rule formula and the results of these properties are summarized in the Tables 4 and 5.

The values given in Table 4 are the calculated properties of the carbon/epoxy composite material with 60% carbon fiber percentage.

Using these mechanical properties of carbon/epoxy and carbon/CNT/epoxy composites summarized in the above two tables, analysis is made for the coil spring by using ANSYS workbench.

4.2.1. Ply Property Analysis. Modeling of the composite material is about the effort taken to model or calculate the stiffness values of the individual lamina. It is widely mentioned by previous scholars that the stiffness of the lamina and laminate is dependent on three major factors, namely,

(1) Orientation of fibers with respect to a common reference axis.

(2) Type of reinforcement used; continuous or discontinuous fiber used.

(3) Volume fraction of the matrix and fiber.

The range of thickness of a lamina created by using unidirectional fibers is about 0.12–0.20 mm, whereas the thickness of a single ply of a woven or braided fabric ranges from about 0.25 to 0.40 mm. To produce a composite structure with a significant thickness, many plies are stacked together to form a composite laminate [90].

4.3. Solid Modeling of Steel Helical Spring. The specific type of vehicle selected for this research is a "Bajaj RE diesel three-wheeler vehicle." The vehicle has a maximum GVW of 702 kg and its Kerb weight is 307 kg. The study is based on the approach that the vehicle is able to carry a maximum of the average weight of four people. The necessary parameters of the coil spring used on vehicles' front suspension system are mentioned in Table 6. Helical springs have the characteristic parameters that affect their behaviors. In addition to the physical properties of its material, the wire diameter

Table 4: Mechanical properties of the carbon/epoxy laminated composite.

No.	Material properties	Symbol	Value
1	Density (g/cm^3)	ρ	1.53
2	Poisson's ratio 12	ν_{12}	0.28
3	Poisson's ratio 23	ν_{23}	0.77
4	Poisson's ratio 13	ν_{13}	0.28
5	Tensile strength 1-direction (GPa)	σt_1	2.64
6	Tensile strength 2-direction (GPa)	σt_2	2.00
7	Tensile strength 3-direction (GPa)	σt_3	2.00
8	Compressive strength in 1-direction (GPa)	σc_1	0.796
9	Compressive strength in 2-direction (GPa)	σc_2	0.384
10	Compressive strength in 3-direction (GPa)	σc_3	0.384
11	Shear modulus in 12-direction (GPa)	G_{12}	7.14
12	Shear modulus in 23-direction (GPa)	G_{23}	3.087
13	Shear modulus in 13-direction (GPa)	G_{13}	7.14
14	Young's modulus 1-direction (GPa)	$E1$	139.38
15	Young's modulus 2-direction (GPa)	$E2$	17.37
16	Young's modulus 3-direction (GPa)	$E3$	17.37

Table 5: Calculated properties of carbon/epoxy with the CNT additive laminated hybrid composite (@ $Vf_2 = 1\%$).

No	Material properties	Symbol	Value
1	Density (g/cm^3)	ρ	1.5
2	Poisson's ratio 12	V_{12}	0.33
3	Poisson's ratio 23	V_{23}	0.78
4	Poisson's ratio 13	V_{13}	0.33
5	Tensile strength 1-direction (GPa)	σt_1	4.144
6	Tensile strength 2-direction (GPa)	σt_2	0.309
7	Tensile strength 3-direction (GPa)	σt_3	0.309
8	Compressive strength in 1-direction (GPa)	σc_1	2.12
9	Compressive strength in 2-direction (GPa)	σc_2	0.384
10	Compressive strength in 3-direction (GPa)	σc_3	0.384
11	Shear modulus in 12-direction (GPa)	G_{12}	7.4
12	Shear modulus in 23-direction (GPa)	G_{23}	5.5
13	Shear modulus in 13-direction (GPa)	G_{13}	7.4
14	Young's modulus 1-direction (GPa)	$E1$	149.08
15	Young's modulus 2-direction (GPa)	$E2$	14
16	Young's modulus 3-direction (GPa)	$E3$	14

Table 6: Existing coil spring parameters.

Existing coil spring parameters		
1	Free length of the spring, L_f	210 mm
2	Core diameter of the spring, Di	42.88 mm
3	Wire diameter of the spring, d	12 mm
4	Outer diameter of the spring, D_o	66.88 mm
5	Number of active coils, N_a	10
6	Total number of turns, N	12

(d), mean diameter (D), number of coils (N), and the pitch (P) are the parameters that affect the behavior of spring.

The three-wheeled vehicle used in this study has the capacity to carry a total of four people, and this vehicle is mostly used in African and some Asian countries. Hence, the load to be used in the design is chosen by considering the average body mass of the population in these two continents. As it has been previously studied by other researchers [91], the average body mass of the African population is 60.7 kg, while it is 57.7 kg for the Asian population.

4.4. Fatigue Loading in Springs. Helical springs are likewise subjected to fluctuating strains in practice. Variable stresses are used in this process. A maximum stress load value and a minimum stress load value exist. According to Gupta and Khurmi, Budynas and Nisbett [92, 93], in the case of designing fatigue-loaded springs, the Soderberg line approach is applied. In most cases, helical springs are only loaded in one direction. As a result, for spring design analysis, the modified Soderberg diagram is employed. The force-deflection characteristic of a helical coil spring is ideally linear. It is approximately so in practice, but not at both ends of the force-deflection curve. The spring force is not repeatable for very tiny deflections, and as the number of active turns decreases and the coils begin to touch, nonlinear behavior emerges. The maximum operational force should be limited to $F_{\max}$ 7/8 F_s because the designer confines the spring's operating point to the middle 75% of the curve between no-load, $F = 0$, and closure, $F = F_s$. Thus, the largest force of operation should be limited to $F_{\max} \leq 7/8F_s$. Based on previously done research studies, the most recommended value for ξ is to be either equal or greater than 0.15; thus, in this case, it will be taken as $\xi = 0.15$.

Therefore,

$$\begin{aligned} F_s &= (1+\xi)F_{\max} \\ &= (1+\xi)\frac{7}{8}F_s \\ &= \mathbf{1810}N. \end{aligned} \tag{17}$$

4.4.1. S-N Curve Fatigue Properties. The term "fatigue loading" refers to a situation in which a material is subjected to both tensile and compressive stresses at the same time. The "SN curve" is a graph that shows the results of fatigue testing. According to [94, 95], the S-N curve appears to still be the most popular method of describing the fatigue behavior of composite materials. These papers state that one of the simpler equations used to describe the fatigue behavior of several composite materials is as follows (Figure 12), while taking σ_a as the maximum applied stress, σ_u as the static strength, b as a constant, and N as the number of cycles to failure.

$$\begin{aligned} \log(\sigma_A) &= \log\left(aN^b\right), \\ \log(\sigma_A) &= \log(a) + b\log(N), \\ \sigma_A &= \sigma_u - b\log N, \\ \text{Where, } b &= \frac{\log\left(S_m/S_e\right)}{\log\left(10^3\right) + \log\left(10^N\right)}. \end{aligned} \tag{18}$$

The type of material used to construct the conventional coil spring is SAE5160 carbon steel, which is the most

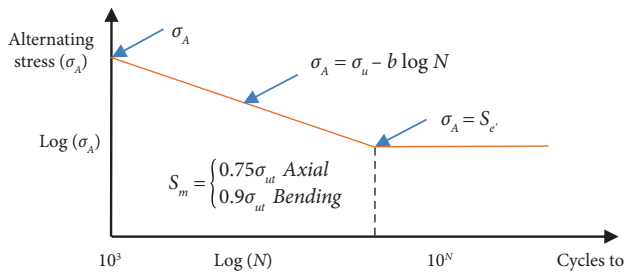

Figure 12: S-N curve representation.

common material in the automobile coil spring industry. Some of the mechanical properties of this material are given in Table 7.

4.4.2. S-N Curve for Carbon/Epoxy Spring. It is calculated that the ultimate strength σ_u for carbon/epoxy composite material is 2.64 GPa.

$$\begin{aligned} S_m &= 0.75\sigma_{ut}, \\ S_m &= 0.75\sigma_{ut} = 1980\,\text{MPa}. \end{aligned} \tag{19}$$

But, as it is indicated on the diagram, $S_m = \sigma_A$ at $N = 10^3$ Hence, the constant (b) can be calculated as follows:

$$\begin{aligned} \sigma_A &= \sigma_u - b \log N, \\ b &= 220. \end{aligned} \tag{20}$$

Therefore, the general S-N curve equation for carbon/epoxy composite material is as follows:

$$\sigma_A = 2640Mpa - 220 \times \log N. \tag{21}$$

Through the same process, the general S-N curve formula for the carbon/CNT/epoxy composite material will be as follows:

$$\sigma_A = 4144Mpa - 345.33 \times \log N. \tag{22}$$

According to the SN curve, equations for the two types of composite materials will be plotted as follows. While plotting, the graph of the logarithmic scales of the axis is used for two major reasons. The first reason is to respond to skewness in large values. For example, when a few of the points from the data are much larger than the bulk, the second reason is to show a change in percentage or multiplicative factors.

The SN curves of the two composite materials are plotted together in Figure 13 to make a clear and easy comparison.

The orange color represents carbon/CNT/epoxy, whereas the black one is for the carbon/epoxy composite. Generally, the graph tells that the carbon/CNT/epoxy composite has a better fatigue life than the carbon/epoxy composite material.

4.4.3. Coil Spring Terminologies. (1) Solid Length (L_s). If the coils of the spring come into contact with each other during compression, the spring is considered to be solid. The solid length of a spring is calculated as the product of the wire

Table 7: Properties of SAE5160 carbon steel [96].

Properties	Values
Modulus of elasticity (Young's modulus), E (GPa)	207
Shear modulus, G (GPa)	80
Yield strength, (MPa)	1487
Ultimate tensile strength, σ_u (MPa)	1584
Fatigue strength coefficient, σ_f' (MPa)	2063
Fatigue strength exponent, b	−0.08
Fatigue ductility coefficient, ε_f'	9.56
Fatigue ductility exponent, c	−1.05

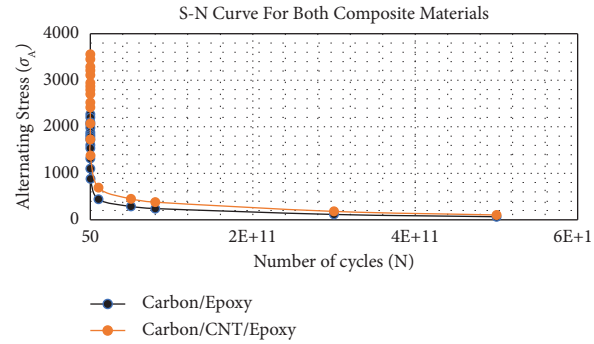

Figure 13: S-N curve comparison of both composites.

diameter and the total number of coils. This is described in the third figure in Figure 14. Mathematically,

$$\begin{aligned} \text{Solid length of the spring, } L_s &= N_t \times d, \\ L_s &= N_t \times d \\ &= 12 \times 12 \\ &= 144\text{mm}, \end{aligned} \tag{23}$$

where N_t = Total number of coils and d = diameter of the wire.

(2) Free Length (L_f). The free or unloaded length of a compression spring is the length of the spring when it is not in a loaded condition, as it is described in Figure 14 (first figure). It can be equated with the solid length plus the maximum compression or deflection of the spring and the clearance in between the adjacent coils (at full compression condition). Mathematically, this is written as follows:

$$L_f = N_t \times d + \delta_{\max} + 0.15\delta_{\max}. \tag{24}$$

The free length of the compression coil spring can also be calculated using the following equation:

$$L_f = N_t \times d + \delta_{\max} + (N - 1) \times 1\text{mm}. \tag{25}$$

In this case, the gap (clearance) between the two adjacent coils is taken as 1 mm.

(3) Spring Rate (K). The spring rate, which is also known as stiffness or spring constant, is the ratio of the applied load to the spring's deflection. This can also be expressed mathematically as follows:

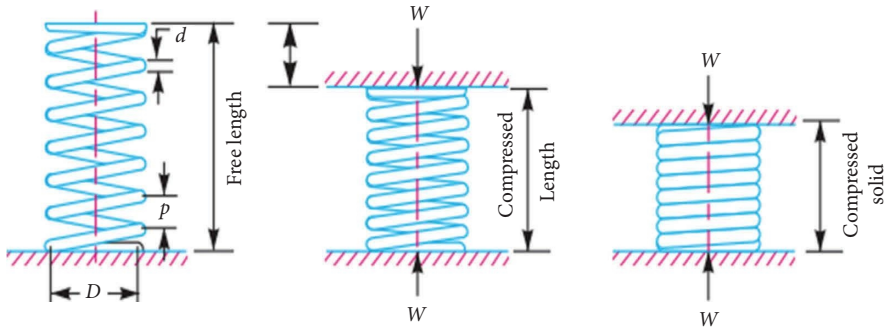

Figure 14: Helical compression coil spring terminologies [93].

$$\text{Spring rate (stiffnes constant)}, K = \frac{F}{\delta}, \tag{26}$$

where F = Load and δ = Deflection of the spring.

(4) Spring Index (C). It is the relationship between the spring's mean diameter and its wire diameter. In general, spring index is the ratio of the mean diameter of the spring to the wire diameter of the spring. Mathematically,

$$\text{Spring index } C = \frac{D_m}{d}, \qquad D_m = D_o - \text{d} = 54.88\text{mm}, \tag{27}$$

where D_m = mean diameter of the coil spring, D_o = outer diameter of the coil spring, and d = wire diameter

For existing coil spring,

$$\text{Spring index } C = \frac{D_m}{d} = 4.57\text{mm}. \tag{28}$$

(5) Pitch (P). The pitch of the spring is the distance between the center of one wire and the center of the adjacent wire of the spring. As displayed in Figure 14, the pitch is the axial distance between adjacent coils in an unloaded (free) state. The pitch of the spring could be determined by using the following formula:

$$\text{Pitch of the coil}, = \frac{\text{Free length}}{N_t - 1}. \tag{29}$$

The pitch of the coil may also be obtained by using the following relation, i.e., pitch of the coil:

$$\text{P} = \frac{L_f - L_s}{N_t} + d = 17.5\text{mm}, \tag{30}$$

where L_f = free length of the spring, L_s = solid length of the spring, N_t = total number of coils, and d = diameter of the wire.

The following two considerations should be considered when choosing the pitch of spring coils, according to Buragohain [88],

(a) The coil pitch should be such that the stress does not raise the yield point tension in torsion if the spring is accidentally or carelessly compressed.

(b) The spring should not close before it reaches its maximum service load.

4.4.4. Deflection and Stiffness Calculation of the Circular Wire Spring. The type of spring used in this research has a circular shaped wire. Therefore, the deflection and stiffness will be calculated by considering the spring wire as having a circular shape. The total strain energy of a helical spring includes two components which are the torsional component and shear component. However, the shear component is insignificant and can be neglected. The strain energy in spring is related to its force and deflection behavior, and the deflection of spring may be approximated using Castiglione's theorem [93].

$$u = \frac{T^2}{2G} \times \frac{L_s}{J} + \frac{F^2}{2A} \times \frac{1}{G}. \tag{31}$$

where $T = F \times D/2$, $L_s = \pi DN$, $J = \pi \times d^4/32$ and $A = \pi \times d^2/4$.

Then, based on Castiglione's theorem, the deflection of a spring can be given as follows:

$$\delta = \left(\frac{8FD_m{}^3N_a}{Gd^4}\right)\left(1 + \frac{1}{2C^2}\right), \tag{32}$$

Here, N_a is the number of active coils.

Therefore, using this general formula, the deflection of the three springs will be as follows:

$$\delta_{(\text{steel spring})} = 15.277\text{mm}, \quad \delta\left(\frac{\text{Carbon}}{\text{Epoxy Spring}}\right) = 165.534\text{ mm}, \quad \delta\left(\frac{\text{Carbon}}{\text{CNT/Epoxy Spring}}\right) = 159.718\text{ mm}. \tag{33}$$

In this case, the deflection comparison for these three different material springs is made using the existing spring dimensions. So, the results at designing load are 15.277 mm, 159.71 mm, and 165.53 mm for steel, carbon/CNT/epoxy, and carbon/epoxy composite, respectively. Similarly, the deflection values of existing spring and composite springs at different loading conditions are calculated.

We can deduct from these findings that composite materials are far more deformable than steel. Using these composites directly without modification or parameter changes made either to the material itself or to the coil spring will not work the way it is intended. Therefore, the first target of this research paper is to optimize design variables (wire diameter, number of coils, and mean diameter of the coil spring) in the coil spring, which could maximize the spring's performance and allow for acceptable outcomes. The parameters to be used for this study in reducing deformation are decreasing mean diameter, increasing wire diameter, or reducing the number of coils. So, this study finds a better and more acceptable result by replacing the existing steel spring with a composite spring, which could be lighter in weight but still have good performance for light vehicles.

5. Modeling and Analysis

The coil spring is modeled using SOLIDWORKS 2018 modeling software based on the calculated coil spring parameters as well as direct measurements. The developed model is saved in STEP or IGES file format and then is analyzed under uniform loading condition in ANSYS workbench R19.2. Axial displacement and shear stress have been compared with analytical results. Load is in direction of spring axis and is exerted on the one end of spring and other end is fixed in X, Y and Z directions. Meshes with different resolutions are generated to insure grid independence.

Figure 15 shows the existing helical coil spring which is modeled using SOLIDWORKS 2018 solid modeling CAD and CAE computer program. The dimensions directly measured from the real coil spring (disassembled from the BAJAJ RE vehicle) as well as dimensions that are calculated using standard coil spring design formulas are also considered.

5.1. Boundary Conditions for Static Analysis. Boundary conditions are constraints that must be met in order to solve a boundary value problem. As a result, the restrictions required for static analysis of helical coil springs are exhibited in Figure 16. On one end of the spring, a load of 1810N is applied, and fixed support is taken on the other.

For static analysis, the load is applied on the top of one end of the coil spring, and the other end is constrained as a fixed support. Figure 16 shows two boundary conditions (A and B) applied to the spring. In the figure, the boundary condition marked with the letter A (blue-colored) is the fixed support boundary condition and the one symbolized by the letter B (red-colored) is the load boundary condition.

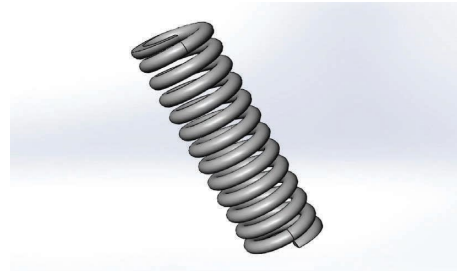

Figure 15: Existing coil spring model prepared by SOLIDWORKS 2018.

5.2. Meshing. Meshing is a technique in the computer-aided engineering (CAE) simulation process that converts irregular forms into discrete, recognizable volumes called elements. In FEA, meshing has an impact on the solution's accuracy, convergence, and speed. The hexahedral element meshing method is used in this study as it can provide more accurate results at lower element counts and it has been selected for complex geometries in many researches. For better quality and an accurate analysis result, first results are checked at different mesh qualities and the elements' size is refined until the results are independent of mesh size and stops changing. From literature reviews, the two well-known convergence criteria or methods of improving finite element analysis are "P"–convergence and "H" convergence. From these two methods, the "H" type convergence method is used in this research for mesh refinement [97, 98]. The mesh is made to converge for better response with a suitable tolerance limit and the elements shape quality is also considered. According to this, the selected better quality and fine mesh size is $1.89e-003$ m which consists of 183325 nodes and 100941 elements for existing coil spring. The generated mesh for coil spring is given in Figure 17.

6. Results and Discussion

The model of the coil spring has been set to the boundary conditions, and meshing has also been done in a way that can give us a good result. Then, the model is tested for maximum shear stress, deformation, equivalent stress, and strain effects at various applied loads. Similarly, the modified coil spring is also tested for these properties under the same boundary conditions. The results of these properties for both modified and existing coil springs are discussed and tabulated and also given in graphs to make their difference easily noticeable and for clear comparison. In this study, both the analytical and FEA methods are used, and the results of both types are also given comparatively. FEA can yield spectacularly accurate results. However, it highly depends on the quality of model construction and the boundary conditions used for the analysis. The analytical hand calculation is also adequate for the complete analysis of simpler problems. Combining the two methods is often used because it provides a good starting point for design, which can then be further optimized with FEA. Hand calculations are also used to validate FEA results and determine the accuracy of the model.

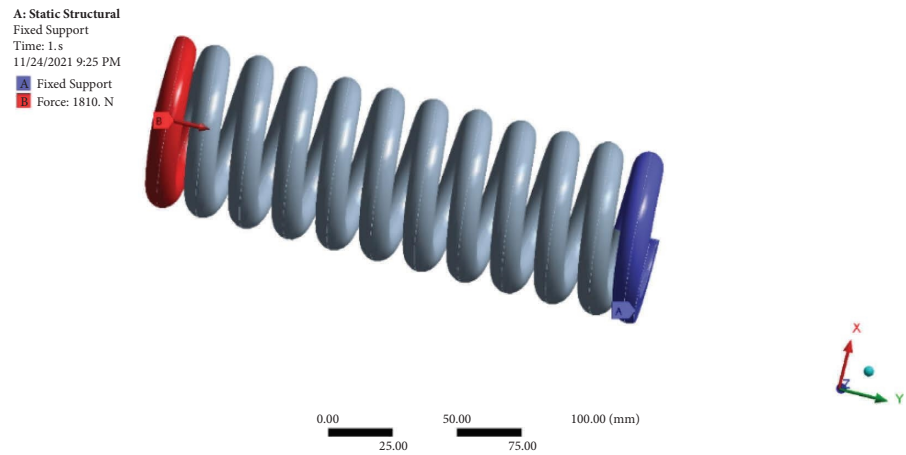

Figure 16: Boundary conditions for static analysis of a coil spring.

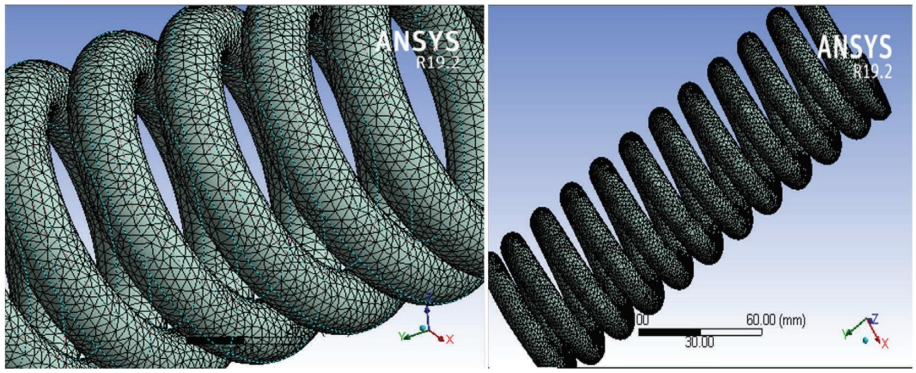

Figure 17: Meshing of coil spring.

6.1. Coil Spring Deformation Results. The deformation analysis results are tabulated in Table 10 below for the steel material as well as carbon/CNT/epoxy and carbon/epoxy composite materials.

The results show that the composite material springs have a much larger deflection when compared with the same dimension steel spring. Especially for very large loads, the deformation of the composite spring is very large. Therefore, this leads to the conclusion that composite materials cannot be of good enough performance to be used as spring materials unless some parameter optimization is done. This property of the composite materials has also been verified by different scholars stated in the introduction section. The above results are compared and explained using graphs in Figure 18.

The lines of different colors represent the deflection versus load graph of the individual spring types. The line colored in green represents load versus deflection values of steel coil springs, while the yellow and blue-colored lines indicate carbon/CNT/epoxy and carbon/epoxy composite springs, respectively. The deflection difference between these springs is clear and visible in the graph. Hence, the composite springs are more deformed than the existing steel springs. And comparing the two composite springs, the carbon/CNT/epoxy deforms less than the carbon/epoxy spring. As a result, design variables such as wire diameter of

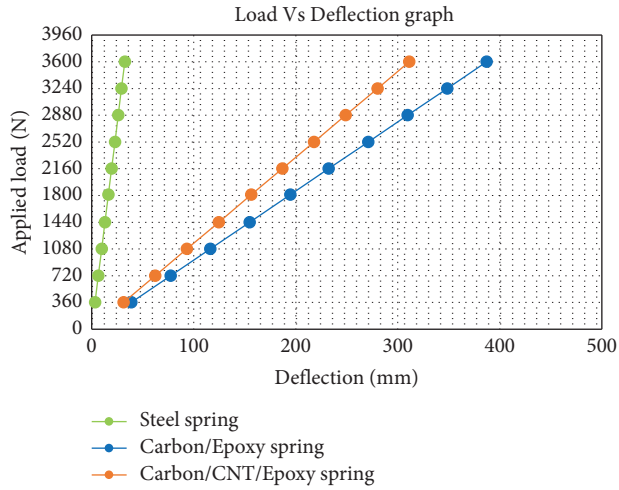

Figure 18: Load vs deflection graph of the springs.

the spring, number of coils, and mean diameter are redesigned. Again, these newly designed springs are analyzed to see if the performance can be up to the acceptable label or not. So, the results of the analysis of the modified spring are given in Table 8. It contains both the analytical and FEA results of the three material types of springs. In this case, the results for steel-made springs are taken with the existing

Table 8: Comparison of deflection of the modified composite coil spring with steel spring model.

Load (N)	Deflection of the spring (mm)					
	Steel spring		Carbon/epoxy spring		Carbon/CNT/epoxy spring	
	Analytical	FEA	Analytical	FEA	Analytical	FEA
360	3.039	3.249	2.924	3.72	2.821	2.9839
720	6.077	6.499	5.848	7.44	5.643	5.9678
1080	9.116	9.748	8.773	11.16	8.464	8.9518
1440	12.154	12.997	11.697	14.88	11.286	11.936
1810	15.277	16.336	14.702	18.703	14.186	15.003
2160	18.232	19.495	17.545	22.32	16.929	17.904
2520	21.270	22.745	20.470	26.04	19.750	20.887
2880	24.309	25.994	23.394	29.76	22.572	23.871
3240	27.347	29.234	26.318	33.48	25.393	26.855
3600	30.386	32.492	29.242	37.2	28.215	29.839

dimensional values to make the comparison with the optimized carbon/epoxy and carbon/CNT/epoxy springs.

These results show that the modified springs are improved and their deflection is decreased when compared with their previous versions. And the carbon/CNT/epoxy composite spring has the least deformation than the carbon/epoxy composite spring and existing steel coil spring but carbon/epoxy spring has still larger deflection than the existing steel spring at the same loading conditions, i.e., at the designing load (1810 N), the deflection values are 16.336, 18.703, and 15.003 mm for steel, carbon/epoxy, and carbon/CNT/epoxy springs, respectively. The results, in the form of a load versus deflection graph, are presented in Figure 19.

The graphs in Figure 19 clearly show that the maximum deflection, which was the limitation of the unmodified spring, is now improved enough, so that after modification of parameters, the deformation of the carbon/CNT/epoxy composite spring is less than both the carbon/epoxy composite and steel springs.

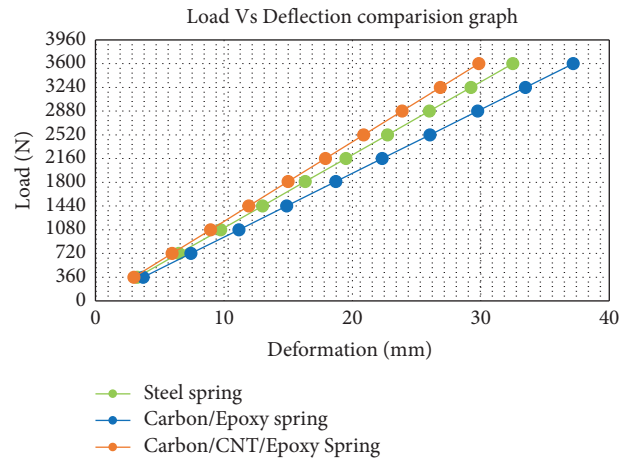

Figure 19: Load versus deflection for modified coil spring.

6.2. Maximum Shear Stress Results. The maximum shear stress analyses are done for existing and modified designs, and the results of those spring designs are tabulated in Table 9 for comparison at variable loading conditions.

These analysis results are also clearly described in Figure 20. The table as well as the figure shows that the maximum shear stress of the composite springs, which is designed to the same dimension as the existing spring, has a higher maximum shear stress than the existing steel spring.

For example, at the designing load (1810 N), the maximum shear stress of the steel spring is 205.5 MPa, and it is 240.83 MPa and 228.72 MPa for the carbon/epoxy and carbon/CNT/epoxy composite springs. Table 10 also shows that the maximum shear stress values are similar for three different material springs, which means that the springs are not highly dependent on the type of material from which they are made but force-dependent. The figure shows that as axial compression load increases, maximum shear stress also increases. According to the above results, the selected composite materials cannot replace the existing steel material for springs for the same spring parameters. Therefore, optimization of spring parameters is required for the composite-made springs and they will be tested again. The existing coil spring is optimized by changing design variables such as spring wire diameter and number of total and active number of coils. Hence, maximum shear stress analyses are done for carbon/epoxy and carbon/CNT/epoxy-modified composite springs and the results are shown in Table 11.

Both the analytical and FEA results in Table 11 show that the modified spring has a lower shear stress value than the existing springs at different loading conditions, which is a highly required property for the optimization of the spring. In addition to the lower deflection for similar loading conditions, the new spring has a low shear stress value. Despite the differences in materials, the analytical values of the two composite springs are identical. This indicates that the shear stress of springs is unaffected by the type of material used, but the table also indicates that the maximum shear stress is determined by the spring's geometrical dimensions. These are also described in Figure 21, which clearly depict the changes.

The graph shows that both optimized composite springs have lower shear stress values when compared with the existing steel spring, and of the two modified composite springs, the carbon/CNT/epoxy spring has a lower maximum shear stress value than the carbon/epoxy spring. Therefore, from the shear stress perspective, the carbon/CNT/epoxy spring type is still the best one. The graph also

Table 9: Maximum shear stress values of steel, carbon/epoxy, and carbon/CNT/epoxy springs using existing spring dimensions.

Load (N)	Maximum shear stress (MPa)					
	Steel spring		Carbon/epoxy spring		Carbon/CNT/epoxy spring	
	FEA	Analytical	FEA	Analytical	FEA	Analytical
360	40.872	39.17916	47.9	39.17916	45.491	39.17916
720	81.7465	78.35832	95.799	78.35832	90.983	78.35832
1080	122.62	117.53748	143.7	117.53748	136.47	117.53748
1440	163.49	156.71664	191.6	156.71664	181.97	156.71664
1810	205.5	196.98411	240.83	196.98411	228.72	196.98411
2160	245.23	235.07496	287.4	235.07496	272.95	235.07496
2520	286.11	274.25412	335.3	274.25412	318.44	274.25412
2880	326.98	313.43328	383.2	313.43328	363.93	313.43328
3240	367.85	352.61244	431.1	352.61244	409.42	352.61244
3600	408.72	391.79160	479	391.79160	454.91	391.7916

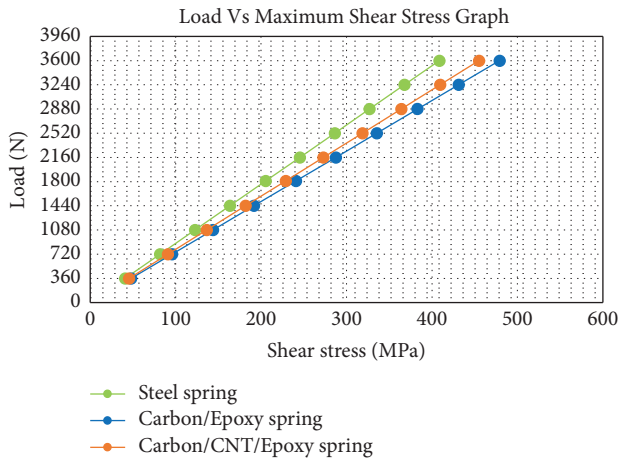

Figure 20: Load versus shear stress comparison of steel spring with composite springs of the same dimension.

Table 10: Analytical and FEA values' comparison for three types of coil springs.

Load (N)	Spring deflection (mm)					
	Steel spring		Carbon/epoxy spring		Carbon/CNT/epoxy spring	
	Analytical	FEA	Analytical	FEA	Analytical	FEA
360	3.039	3.249	32.924	38.70	31.767	31.115
720	6.077	6.499	65.848	77.41	63.534	62.231
1080	9.116	9.748	98.772	116.11	95.301	93.346
1440	12.154	12.997	131.696	154.82	127.069	124.46
1810	15.277	16.336	165.534	194.60	159.718	156.44
2160	18.232	19.495	197.544	232.23	190.603	186.69
2520	21.270	22.745	230.467	270.93	222.370	217.81
2880	24.309	25.994	263.391	309.63	254.137	248.92
3240	27.347	29.234	296.315	348.34	285.904	280.04
3600	30.386	32.492	329.239	387.04	317.671	311.15

Table 11: Maximum shear stress comparison of steel with modified composite coil springs.

Load (N)	Maximum shear stress (modified spring) (MPa)					
	Steel spring		Modified Carbon/epoxy spring		Carbon/CNT/epoxy spring	
	FEA	Analytical	FEA	Analytical	FEA	Analytical
360	40.872	39.17916	15.451	11.501	14.456	11.501
720	81.7465	78.35832	30.903	23.001	28.913	23.001
1080	122.62	117.53748	46.354	34.502	43.369	34.502
1440	163.49	156.71664	61.806	46.003	57.825	46.005

Table 11: Continued.

Load (N)	Maximum shear stress (modified spring) (MPa)					
	Modified					
	Steel spring		Carbon/epoxy spring		Carbon/CNT/epoxy spring	
	FEA	Analytical	FEA	Analytical	FEA	Analytical
1810	205.5	196.98411	77.686	57.823	72.683	57.823
2160	245.23	235.07496	92.708	69.004	86.738	69.004
2520	286.11	274.25412	108.16	80.505	101.19	80.505
2880	326.98	313.43328	123.61	92.006	115.65	92.006
3240	367.85	352.61244	139.06	103.50	130.11	103.51
3600	408.72	391.79160	154.51	115.00	144.56	115.01

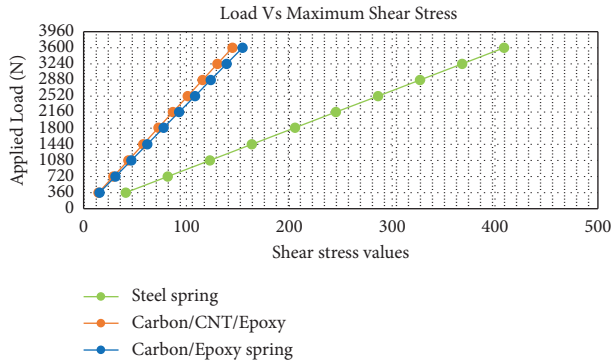

Figure 21: Maximum shear stress comparison of the modified coil spring model with an existing spring.

shows that the shear stress value of the helical spring decreases as the wire diameter increases and the mean diameter decreases.

6.3. Strain Energy. Strain energy is the capacity of the spring to return to its initial position after deformation due to road irregularity or roughness. Hence, the spring design is required to consider and attain higher strain energy. The strain energy of a material is dependent on density, Young's modulus, and induced stress. A material that has a higher density and Young's modulus will have smaller strain energy. This property of materials is shown in Table 12 by using variable loads to compare the corresponding strain energy values of the three types of springs.

Table 12 shows that the strain energy values of the two composite material springs are higher than the existing steel spring at all given loading conditions. Therefore, carbon/epoxy and carbon/CNT/epoxy composite springs are better suited to attain the required quality of absorbing shocks and retaining their original position after deformation. All the results in Table 12 are given and compared using graphs on Figure 22.

A strain energy analysis is also done for the optimized composite springs and the results are given in Table 13 in comparison with the corresponding results of the steel spring.

So, the graphs in Figure 23 indicate that the strain energy is improved in modified springs when compared with the existing ones.

Table 12: Strain energy comparison for the existing spring model.

Load (N)	Strain energy for the existing spring model (mJ)		
	Steel spring	Carbon/epoxy spring	Carbon/CNT/epoxy spring
360	0.059575	0.6167	0.3930
720	0.2383	2.4671	1.5722
1080	0.53617	5.5510	3.5373
1440	0.9532	9.8685	6.2886
1810	1.506	15.591	9.9354
2160	2.1447	22.204	14.149
2520	2.9192	30.222	19.259
2880	3.8128	39.474	25.154
3240	4.8256	49.959	31.836
3600	5.9575	61.678	39.304

The graph (Figure 23) as well as Table 13 displays that the modified carbon/epoxy and carbon/CNT/epoxy composite springs have better strain energy than the existing steel springs. Therefore, in this aspect, these two composite materials can be preferred as construction materials for springs (Table 14).

Summary of the results for deformation, maximum shear stress, and strain energy at a design load of 1810 N are given in Table 14 and results of modified and existing dimension springs are compared using charts.

The deflection of the existing steel spring and the two composite material springs are compared at the design load (1810 N) as shown in Figure 24. Based on the figure, the composite spring with no modification has a larger deformation value than the existing steel spring, but after

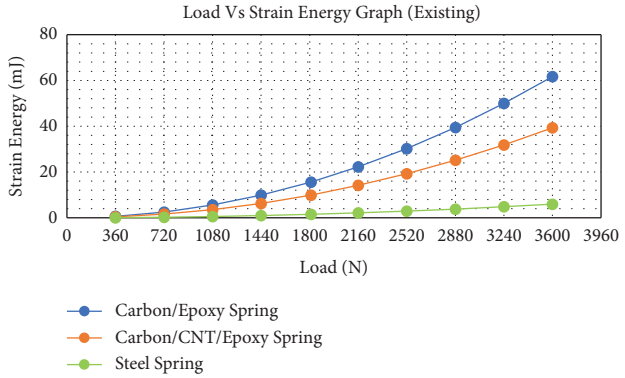

Figure 22: Load versus strain energy comparison.

Table 13: Strain energy comparison for modified spring model.

Load (N)	Strain energy values (mJ)		
	Existing steel spring	Modified	
		Carbon/epoxy spring	Carbon/CNT/epoxy spring
360	0.0595	0.1408	0.0935
720	0.2383	0.5635	0.3741
1080	0.5361	1.268	0.8418
1440	0.9532	2.2543	1.4966
1810	1.506	3.5616	2.3644
2160	2.1447	5.0721	3.3672
2520	2.9192	6.9037	4.5832
2880	3.8128	9.0171	5.9862
3240	4.8256	11.412	7.5763
3600	5.9575	14.089	9.3534

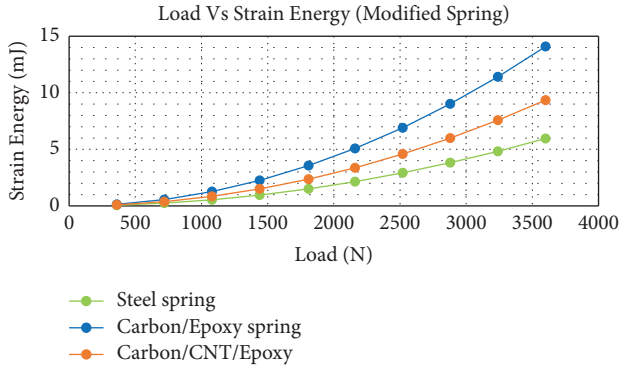

Figure 23: Strain energy graph comparison for modified spring model.

Table 14: Summary of results at a designing load (1810N).

Spring types	Properties	Results	
		Existing spring	Modified spring
Steel spring	Deformation	16.336	—
	Max. shear stress	205.5	—
	Strain energy	1.506	—
Carbon/epoxy spring	Deformation	194.60	18.703
	Max. shear stress	240.83	77.686
	Strain energy	15.591	3.5616
Carbon/CNT/epoxy spring	Deformation	156.44	15.003
	Max. shear stress	228.72	72.683
	Strain energy	9.9354	2.3644

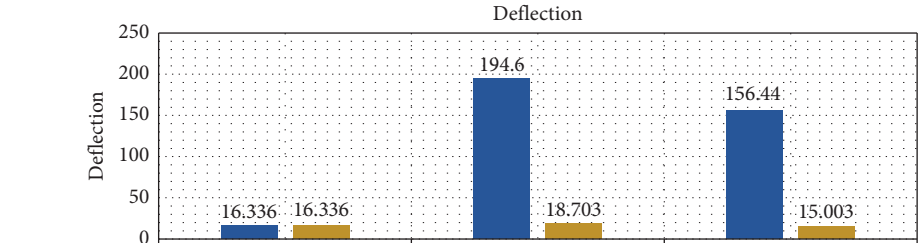

Figure 24: Deflection of composite springs with existing steel spring.

modification of spring parameters, the carbon/CNT/epoxy composite spring deforms less when compared with the other two types of springs, and the deformation of the carbon/epoxy spring is still the largest.

At the designing load, it is shown in Figure 25 that the existing steel spring has higher maximum shear stress than the two composite springs for both existing spring dimensions and for modified spring types. Of the two modified spring types, the carbon/CNT/epoxy composite spring has less maximum shear stress than the carbon/epoxy spring.

The strain energy values for both modified and existing springs for the three springs are presented in Figure 26. When the existing spring parameters are considered, the carbon/epoxy spring has the maximum strain energy value, and carbon/CNT/epoxy spring and steel spring have the second and third maximum strain energy values, respectively. After modification of spring parameters, the strain energy of composite springs decreases, but both results are still greater than the strain energy of existing steel springs.

6.4. Mass Comparison. According to the Figure 27, both composite springs have much less mass than the existing steel spring. The mass of the modified composite springs is also described in comparison with their unmodified version. Even if the mass of modified composite springs is greater than that of unmodified composite springs, they are still lighter than existing steel springs. The carbon/CNT/epoxy spring weighs less than the carbon/epoxy spring. Generally, the mass of composite springs deviates more compared with steel springs, which shows the best quality of composites in weight optimization.

6.5. Stiffness. The stiffness of a component refers to how it bends under load while maintaining its original shape once the load is removed. Stiffness is connected with elastic deformation because the component dimensions remain unchanged after the load is removed. The stiffness of a metal is determined by its modulus of elasticity, also known as Young's Modulus, which is constant. The spring constant is the proportional constant k. It is a measurement of how stiff spring is. When a spring is stretched or compressed to a length x different from its equilibrium length, it produces a force $F = -kx$ in the direction of its equilibrium position. Therefore, in this study, the stiffness of the optimized springs is calculated using the hooks formula and listed in Table 15 for comparison with the stiffness of the existing spring.

$$\text{Stiffness} = \frac{\text{Load}}{\text{Deflection}}. \tag{34}$$

These stiffness values of the spring are described in the chart in Figure 28. So, as indicated on the table and figure, the stiffness of the steel spring was the highest when compared with the unmodified dimension composite springs. But after the spring's parameters are redesigned, the carbon/CNT/epoxy composite spring got the highest spring stiffness, whereas in the carbon/epoxy spring, even if its stiffness improved from when compared with its previous version, it could not be better than the steel spring.

6.6. Fatigue Life. The spring's fatigue life is the life expectancy that the spring had before taking a set or breaking during deformation. Spring fatigue is an issue springs face when subjected to cyclic loading, the redundant application of stress, and loads to the material's structural components. For suspension coil springs, this would imply an application in which they are subjected to varying or continuous loads, causing them to compress and recover periodically over their lifetime. Therefore, for compression of springs, fatigue analysis is crucial since the task that springs are involved in is full of continuously repeated vibration. In this study, the stress life approach is used to determine the fatigue life of the composite springs. The fatigue limit or the S-N curve (Wohler curve, fatigue curve) is commonly used to explain the fatigue properties of materials. The S-N curve depicts the relationship between the amplitude of cyclic stress and the number of cycles till failure. Therefore, the S-N curves are plotted based on the calculated values using SN curve equations (32) and (33), respectively, for carbon/epoxy and carbon/CNT/epoxy spring materials as shown in Figure 29.

The plots in these figures clearly show the magnitude of alternating stress versus the number of cycles to failure for the steel (a) as well as the composite materials (b). In this graph, the orange color represents carbon/CNT/epoxy, whereas the black one is for carbon/epoxy composite. Generally, the SN curve graphs above shows the comparison of the S-N curves of the three materials which again depicts

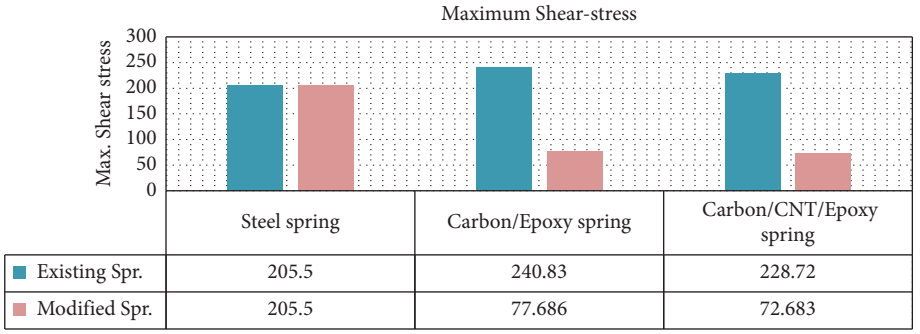

Figure 25: Maximum shear stress comparison of the composite springs with existing steel spring.

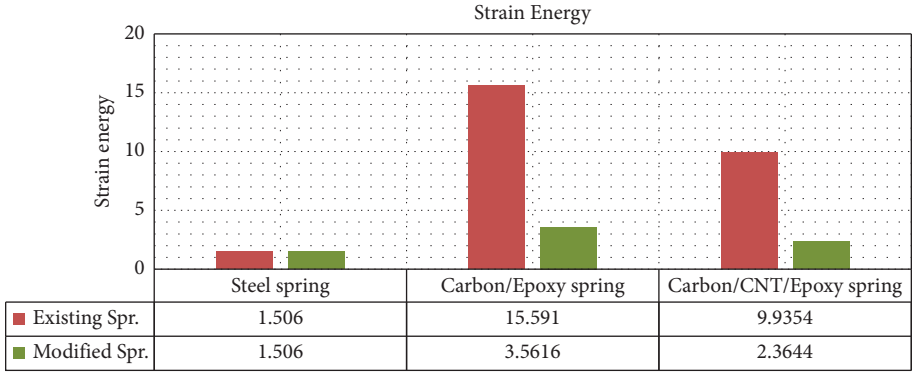

Figure 26: Strain energy comparison of the composite springs with steel spring.

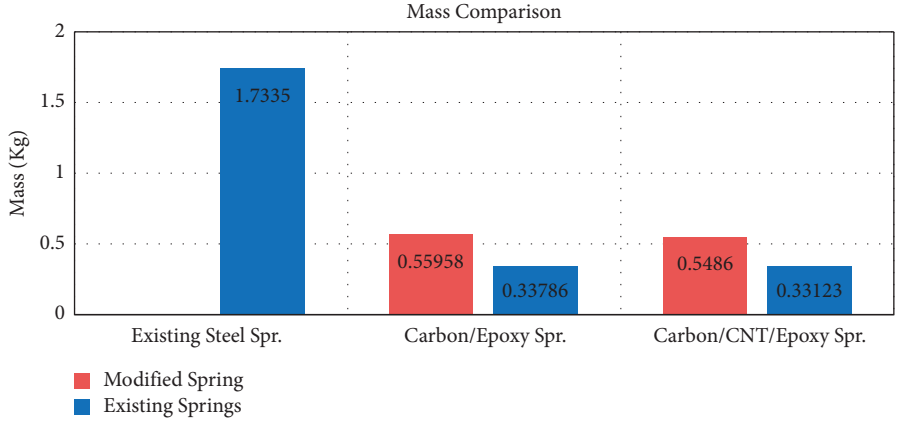

Figure 27: Mass comparison of both composite material springs with the steel spring.

Table 15: Stiffness of existing and modified springs.

	Types of springs		
	Steel coil spring	Carbon/epoxy coil spring	Carbon/CNT/epoxy coil spring
Existing	110.79	9.300	11.570
Modified	110.79	18.70	120.64

the fatigue life of the spring types. Therefore, according to the S-N curves, the carbon/CNT/epoxy composite has a better fatigue life than carbon/epoxy composite and steel materials.

6.7. Dynamic Analysis of Composite Springs. If the application model involves quickly changing loads, considerable accelerating or decelerating motions will be generated, resulting in inertial forces that must be captured using

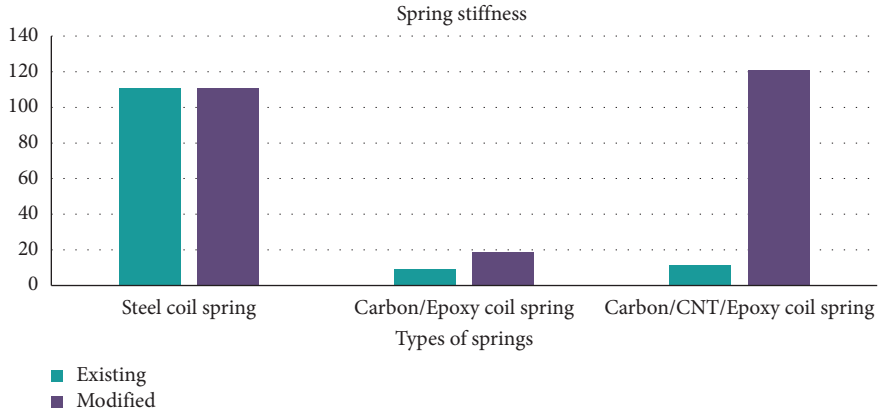

Figure 28: Comparison of the stiffness of the springs.

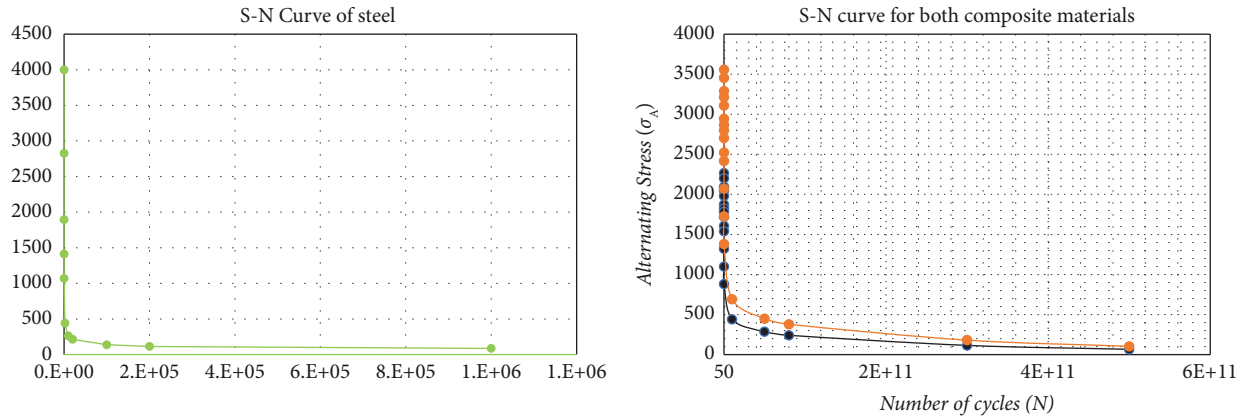

Figure 29: S-N curve of the steel material (a) and composite material (b).

dynamic analysis. Impact loading, for example, drop testing or shock analysis, or vibration motion caused by harmonic loading, are some of the conditions that need dynamic analyses. Dynamic analysis can also accurately capture resonant behavior and transients when they are experienced. Therefore, in this paper, dynamic analysis is used to study the behavior and effect of the spring as it is under dynamic conditions like shock and vibration. Two dynamic analysis types are used for studying the dynamic behavior of the composite spring, namely modal analysis and harmonic analysis. Harmonic analysis determines the steady-state behavior of a structure subjected to cyclic stresses, whereas modal analysis determines the mode frequencies and mode shapes of structures.

6.7.1. Modal Analysis. Modal analysis is a powerful and fundamental type of dynamic analysis, providing the natural frequencies and mode shapes at which a structure will resonate or the dynamic characteristics of structures. Modal analysis is the way to provide information on how the design may respond to different types of dynamic loading. Additionally, it can also serve as a starting point for another, more detailed, dynamic analysis, such as a harmonic response or full transient dynamic analysis.

In this study, modal analysis is used to identify the natural frequency of the new composite spring at a design load, which is again used to check if resonance happens on the spring during vibrational or dynamic loading conditions. Therefore, in this section of the study about dynamic analysis, first, the modal analysis is done, and the natural frequency of the selected spring is determined, then the harmonic analysis is done to evaluate the spring for resonance at the designing load.

In a compression spring, resonance occurs when the cyclic loading frequency is close to or a multiple of the natural spring frequency. Resonance makes individual coil deflection and stress levels increase well beyond what static or equilibrium analysis predicts. Spring bounce can also be caused by resonance, resulting in loads that are significantly lower than those estimated at the minimum spring deflection. To prevent the resonance of the compression springs during dynamic condition loading, the natural spring frequency should be much higher than the operational frequency. In other words, for vibration isolation, the natural frequency of the system should be as far as possible

from the disturbing frequency. The model of the carbon/CNT/epoxy composite spring was inserted into the ANSYS modal analysis workbench and the boundary conditions for modal analysis were set up. In the analysis, all the necessary boundary conditions are applied properly. A fine mesh of 1.89 mm element size is taken and the analysis setting was set to find 10 maximum modes.

For modal analysis, a fixed support is an important boundary condition. Therefore, during the analysis, both the upper and lower ends of the spring are taken as fixed as they are in the real vehicle spring installation. Figure 30 shows the fixed boundary conditions used for modal analysis. The load boundary condition is not considered for modal analysis as it is not necessary for the case. The analysis is completed, and the natural frequency values for ten modes are shown in Table 16.

The natural frequency values of the carbon/CNT/epoxy spring are stated in Table 16 so that these values will be used for comparison with the results from harmonic analysis. The harmonic analysis of a similar spring will be done in the next section, and the result will be taken into evaluation in comparison with the natural frequency values. Consequently, the spring will be tested for resonance. In general, the frequency of the cyclic loading (operating frequency) should be lower than the natural frequency as much as possible.

6.7.2. Harmonic Analysis (Frequency Response). Harmonic response analysis is a type of linear dynamic analysis that is used to figure out how a system reacts to stimuli at various frequencies. Frequency response analysis is another name for it. A modal analysis is required before a harmonic response analysis is performed, as the input frequencies for a harmonic response analysis are the findings of a modal analysis. Harmonic response analysis is a sort of restart analysis that uses modal superposition to calculate its results since it uses previously obtained results. So, in this study, the values recorded in the modal analysis are used to be compared and to conclude the harmonic analysis results.

The harmonic analysis in this paper is done for the new composite (carbon/CNT/epoxy) spring. For this analysis, the required parameters have been fed into the ANSYS harmonic response workbench, and all the necessary boundary conditions have been set. Unlike in modal analysis, here, in harmonic analysis, the load boundary condition is important and this load is called the excitation load. As a result, as shown in Figure 31, the design load of 1810 N is applied to one end of the spring.

The meshing type and the element size (1.98 mm) are taken to be the same as in modal analysis. In the setting of the analysis, the solution interval and the maximum frequency range are taken as 50 and 1000 Hz, respectively. In the damping control option, the structural damping coefficient is set to be 0.25, and this is according to Table 17, which is based on literature papers that were selected for the design of a comfortable vehicle.

In the solution section, the analysis is set to generate the total deformation and the frequency response results. Finally, the frequency response results are generated in both graph and tabular form, with the results in this section including frequencies up to 1000 Hz and their corresponding amplitude values, as shown in Table 18.

These amplitudes and corresponding frequency values are also shown using graph in Figure 32. This figure also shows the frequency value for the maximum amplitude at the excitation force loading.

Both the Table 18 and Figure 32 show the maximum amplitude in the analysis of the spring is 37.15 mm, and the corresponding frequency value is 100 Hz. This value is the excitation or critical frequency at which the spring will have its maximum loading condition (at the excitation load), and this frequency should be much lower than the natural frequency of the spring. From the modal analysis, the natural frequency was determined. The harmonic value should not match or even be close to the natural frequency values. Considering this, the generated values show that the natural frequency of the spring is neither smaller nor closer to the excitation frequency of the spring at the designed load, which means the spring is capable of working in dynamic or harmonic loading conditions.

6.8. Comparison with Previous Works. Up to the submission of this paper, there was no experimental research found that uses exactly the same material used in this study for suspension spring construction. But for general validation, some of the similar or related researches papers are used. From the previously made articles about the suspension coil spring on three-wheeler vehicles, the most related and recent publication is selected from Scopus indexed publishers. The first more related publication is titled as "Optimization of three-wheeler front suspension coil spring" which is studied by Pawar and Desale [99]. The author used the three-wheeler suspension spring which is made of IS-4454 material for the study. The static analysis using finite element method has been done in order to find out the detailed load vs defection of the spring. The study optimizes the spring by reducing total number of turns and experimental investigation was performed to calculate the stiffness and vertical acceleration of helical compression spring. The theoretical calculations were also done. For experimental test, the universal testing machine was used to find load vs defection of spring and quarter car test rig used to find the vertical acceleration of helical compression spring. The study validated the software output by experimental results and found it in a good relation. Finally, the study proves that the optimized spring is better after comparison with other samples. In this research, the previous related works are studied and similar methodologies are taken for comparison; even if the materials used are different, the methods used and the spring parameters are almost the same.

First, the selected recent research is studied and the software analysis is also done similarly using the methodologies used on the paper; then, the results are checked if they are similar with already done on the paper. Some simulation requirements that are not clearly expressed in the validation paper were taken with approximated assumptions by general FEA understandings. Therefore, the results were

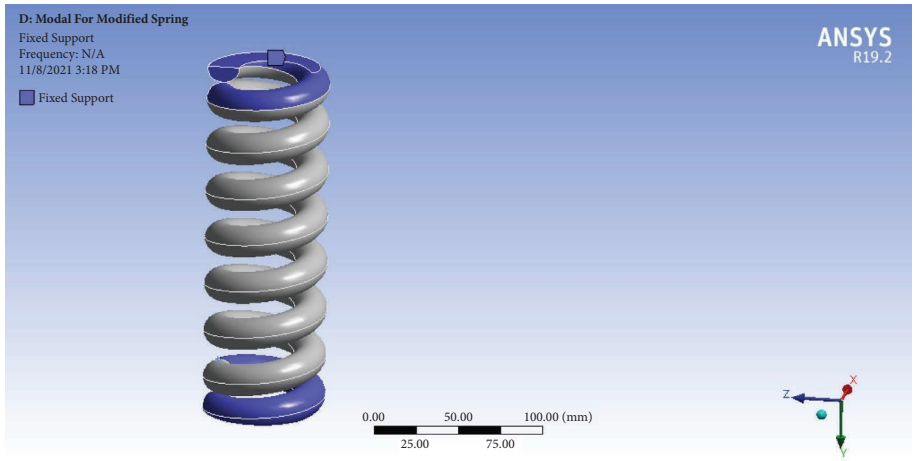

Figure 30: Fixed boundary condition.

Table 16: Natural frequency results from modal analysis.

Modal analysis result	
Mode	Frequency (Hz)
1	229.15
2	270.56
3	315.89
4	324.34
5	488.85
6	531.18
7	611.58
8	663.40
9	754.77
10	778.72

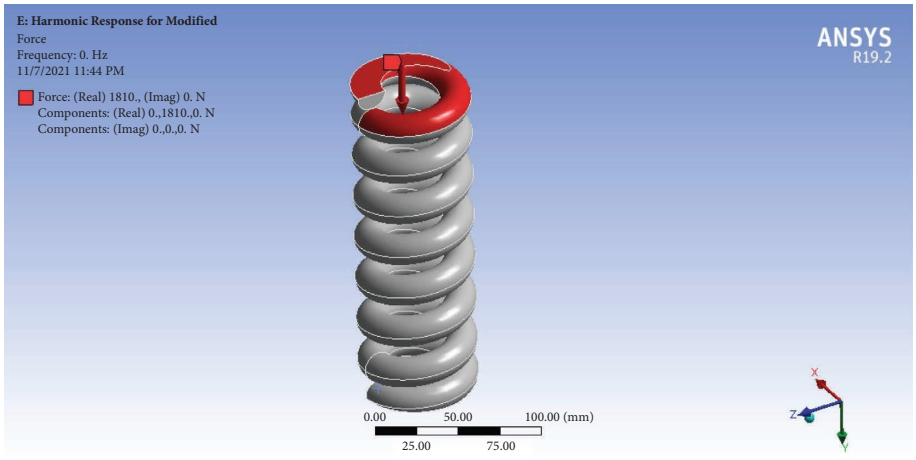

Figure 31: Load boundary condition on the spring.

found to be almost similar but with tolerable deviations. To evaluate the optimized spring model of this study, the spring is brought into the boundary conditions and model that is used in the validation paper and the results are compared.

From the previous studies conducted on the spring which has almost the same spring parameters as the one used in this study, the experimentally proved deflection result for the selected spring is 40 mm at a load of 2000 N. At a similar loading condition, the deflection of the optimized spring in this study is 16.577 mm, which is a highly improved and better result. The experimental shear stress at the spring in the previous study loaded at 2000 N was 420.85 MPa and the corresponding result in this study was 69.502 MPa, which is much better than the previous studies' results.

Table 17: Damping coefficient values for different car types.

Car type	Damping coefficient
Comfortable car	0.20–0.25
Semisport car	0.25–0.30
Sport car	0.30–0.35
Racing car	0.35–0.40

Table 18: Results of harmonic analysis.

Harmonic analysis result (frequency response)	
Frequency (Hz)	Amplitude (mm)
20	9.8795
40	10.535
60	13.412
80	20.388
100	37.15
120	21.462
140	10.967
160	6.8534
180	4.8212
200	3.6751
220	2.9523
240	2.4702
260	2.1389
280	1.8717
300	1.5148

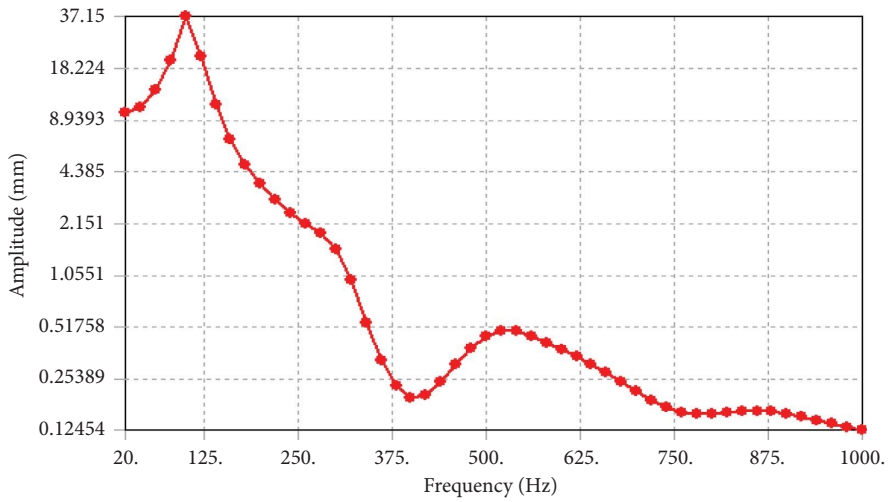

Figure 32: Frequency versus amplitude graph (graphical output form harmonic analysis).

Therefore, the results in this study are roughly validated with those similar previous research papers. The optimized spring properties in this study are found better when compared with those in the previous studies. Therefore, it can be concluded that the optimized Carbon/CNT/Epoxy spring is a good replacement of the existing conventional steel coil springs with additional advantages.

7. Conclusions and Recommendations

Lightweight three-wheeler vehicles can significantly benefit from using composite materials for their front suspension coil springs. This research demonstrates the effectiveness of replacing conventional steel springs with optimized composite springs made of carbon/CNT/epoxy.

Key findings:

(1) Reduced deformation: The modified composite spring showed an 8.16% decrease in deformation compared to the steel spring.

(2) Lower maximum shear stress: Both composite springs exhibited lower shear stress than the steel spring, with the carbon/CNT/epoxy spring boasting a significant 55.42% reduction.

(3) Improved strain energy: The modified composite spring demonstrated 57% better strain energy compared to the steel counterpart.

(4) Enhanced fatigue life: The carbon/CNT/epoxy spring displayed a longer expected lifespan than the steel spring.

(5) Significant weight reduction: Composite springs were substantially lighter than the steel spring, achieving 80.89% and 68.35% weight reductions for the same size and modified design, respectively.

(6) Increased factor of safety: Composite springs demonstrated a three-fold improvement in the factor of safety compared to steel springs, indicating their superior load-carrying capacity.

(7) Dynamic performance analysis: The carbon/CNT/epoxy spring showed promising results under dynamic loading conditions through modal and harmonic analysis.

Conclusion:

Replacing steel springs with the optimized carbon/CNT/epoxy composite springs offers significant advantages for lightweight three-wheeler vehicles. These benefits include the following:

(1) Improved ride comfort and handling due to reduced deformation

(2) Enhanced structural integrity and fatigue life

(3) Reduced weight for improved fuel efficiency and performance

(4) Increased load-carrying capacity for enhanced safety

This research provides a strong evidence for the potential of composite springs to revolutionize suspension systems in lightweight vehicles, paving the way for a more sustainable and efficient future of transportation.

Data Availability

The data used to support this study are included within the article.

Conflicts of Interest

The authors declare that they have no conflicts of interest.

Acknowledgments

This study was sponsored by Addis Ababa Science and Technology University, Bahir Dar University.

References

[1] K. C. Hulsey, "Car front suspension system components," *Automotive Illustration*, vol. 15, 2015.

[2] J. Theunissen, A. Tota, P. Gruber, M. Dhaens, and A. Sorniotti, "Preview-based techniques for vehicle suspension control: a state-of-the-art review," *Annual Reviews in Control*, vol. 51, 2021.

[3] B. Zhang, C. A. Tan, and T. Dai, "Ride comfort and energy dissipation of vehicle suspension system under non-stationary random road excitation," *Journal of Sound and Vibration*, vol. 511, 2021.

[4] A. Aboazoum, "An overview of the most common vehicle suspension problems," *Brilliance: Research of Artificial Intelligence*, vol. 2, pp. 120–124, 2022.

[5] S. S. Gaikwad and P. S. Kachare, "Static analysis of helical compression spring used in two-wheeler horn," *International Journal of Engineering and Advanced Technology (IJEAT)*, vol. 2, 2020.

[6] T. Little, *Top 7 Reasons Why Springs Fail*, APEX Spring & Stamping Corporation, Walker, MI, USA, 2021, https://apexspring.com/blog/top-7-reasons-why-springs-fail/.

[7] Y. Superior, *Mechanical Spring Issue: Corrosion*, 2017, https://www.yostsuperior.com/mechanical-spring-issue-corrosion/.

[8] G. He, Y. Liu, T. Lacy, and M. Horstemeyer, "A historical review of the traditional methods and the internal state variable theory for modeling composite materials," *Mechanics of Advanced Materials and Structures*, vol. 29, pp. 2617–2638, 2022.

[9] D. Gay, *Composite Materials: Design and Applications*, CRC Press, Boca Raton, FL, USA, 2022.

[10] M. Y. Khalid, Z. U. Arif, W. Ahmed, and H. Arshad, "Recent trends in recycling and reusing techniques of different plastic polymers and their composite materials," *Sustainable Materials and Technologies*, vol. 31, 2022.

[11] G. W. Milton, *The Theory of Composites*, SIAM, Delhi, India, 2022.

[12] J. Ekanthappa, G. Shankar, and M. Gagan, "Fabrication and experimentation of FRP helical spring," *IOP Conference Series: Materials Science and Engineering*, vol. 149, 2016.

[13] W. D. Callister, D. G. Rethwisch, A. Blicblau et al., *Materials Science and Engineering: An Introduction*, wiley, Hoboken, NY, USA, 2021.

[14] T. Ramakrishnan, M. D. Mohan Gift, S. Chitradevi et al., "Study of numerous resins used in polymer matrix composite materials," *Advances in Materials Science and Engineering*, vol. 2022, Article ID 1088926, 2022.

[15] M. Soori, "Advanced composite materials and structures," *Journal of Materials and Engineering Structures*, vol. 2023, 2023.

[16] M. Khan, Y. Abbas, and G. Fares, "Review of high and ultrahigh performance cementitious composites incorporating various combinations of fibers and ultrafines," *Journal of King Saud University-Engineering Sciences*, vol. 29, pp. 339–347, 2017.

[17] R. Punyamurthy, D. Sampathkumar, R. P. G. Ranganagowda, B. Bennehalli, and C. V. Srinivasa, "Mechanical properties of abaca fiber reinforced polypropylene composites: effect of chemical treatment by benzenediazonium chloride," *Journal of King Saud University-Engineering Sciences*, vol. 29, pp. 289–294, 2017.

[18] R. Yadav, "Fabrication, characterization, and optimization selection of ceramic particulate reinforced dental restorative composite materials," *Polymers and Polymer Composites*, vol. 30, 2022.

[19] M. K. Egbo, "A fundamental review on composite materials and some of their applications in biomedical engineering," *Journal of King Saud University- Engineering Sciences*, vol. 33, 2020.

[20] S. Kushwah, S. Parekh, and M. Mangrola, "Optimization of coil spring by finite element analysis method of automobile suspension system using different materials," *Materials Today: Proceedings*, vol. 42, pp. 827–831, 2021.

[21] T. S. Ahmadjonovich, "Properties of composite polymer materials and coatings used in automobiles," *Pedagogical Sciences and Teaching Methods*, vol. 2, pp. 160–168, 2023.

[22] W. Han, J. Zhou, and Q. Shi, "Research progress on enhancement mechanism and mechanical properties of FRP composites reinforced with graphene and carbon nanotubes," *Alexandria Engineering Journal*, vol. 64, pp. 541–579, 2023.

[23] V. Chauhan, T. Kärki, and J. Varis, "Review of natural fiber-reinforced engineering plastic composites, their applications in the transportation sector and processing techniques," *Journal of Thermoplastic Composite Materials*, vol. 35, pp. 1169–1209, 2022.

[24] T. E. Twardowski, *Introduction to Nanocomposite Materials: Properties, Processing, Characterization*, DEStech Publications, Inc, Lancaster, PA, USA, 2007.

[25] V. Nimbagal, N. Banapurmath, A. M. Sajjan, A. Y. Patil, and S. V. Ganachari, "Studies on hybrid bio-nanocomposites for structural applications," *Journal of Materials Engineering and Performance*, vol. 30, pp. 6461–6480, 2021.

[26] V. Tambrallimath, R. Keshavamurthy, S. D. Bavan et al., "Mechanical properties of PC-ABS-based graphene-reinforced polymer nanocomposites fabricated by FDM process," *Polymers*, vol. 13, p. 2951, 2021.

[27] J. Huang, J. Zhou, and M. Liu, "Interphase in polymer nanocomposites," *JACS Au*, vol. 2, pp. 280–291, 2022.

[28] S. Morais, "Advances and applications of carbon nanotubes," *Nanomaterials*, vol. 13, p. 2674, 2023.

[29] H. Ijaz, A. Mahmood, M. M. Abdel-Daim et al., "Review on carbon nanotubes (CNTs) and their chemical and physical characteristics, with particular emphasis on potential applications in biomedicine," *Inorganic Chemistry Communications*, vol. 45, 2023.

[30] F. Mohajer, G. M. Ziarani, A. Badiei, S. Iravani, and R. S. Varma, "MXene-carbon nanotube composites: properties and applications," *Nanomaterials*, vol. 13, p. 345, 2023.

[31] K. Ruan, X. Shi, Y. Zhang, Y. Guo, X. Zhong, and J. Gu, "Electric field induced alignment of functionalized carbon nanotubes inside thermally conductive liquid crystalline polyimide composite films," *Angewandte Chemie*, vol. 135, 2023.

[32] J. H. Koo, *Polymer Nanocomposites*, McGraw-Hill Professional Pub, New York, NY, USA, 2006.

[33] S. H. Din, "Nano-Composites and their Applications: a review," *Characterization and Application of Nanomaterials*, vol. 3, 2020.

[34] S. Zavyalov, A. Pivkina, and J. Schoonman, "Formation and characterization of metal-polymer nanostructured composites," *Solid State Ionics*, vol. 147, pp. 415–419, 2002.

[35] S. Asiri, "Mechanical behavior of helical spring made of composite with and without material property grading under stable load," *Journal of Nanomaterials*, vol. 2022, Article ID 9652966, 2022.

[36] L. Chen, L. Wu, H. Fu, and Y. Tang, "Design and performance evaluation of polymer matrix composite helical springs," *Polymers*, vol. 14, p. 3900, 2022.

[37] L. Chen, W. Xing, L. Wu et al., "Understanding multiple parameters affecting static and dynamic performances of composite helical springs," *Journal of Materials Research and Technology*, vol. 25, 2022.

[38] Q. Jiang, Y. Qiao, F. Zhao et al., "Composite helical spring with s kin core structure: structural design and compression property evaluation," *Polymer Composites*, vol. 42, pp. 1292–1304, 2021.

[39] J. Ke, Z. Y. Wu, Y. S. Liu, Z. Xiang, and X. D. Hu, "Design method, performance investigation and manufacturing process of composite helical springs: a review," *Composite Structures*, vol. 252, 2020.

[40] J. Alao, E. Jaiyeoba, T. Danjuma, O. Abdulwahab, and M. Ahmad, "Assessment of damping effect as applicable to automobile shock absorber systems and related damper systems," *International Journal of Scientific and Engineering Research*, vol. 13, pp. 1128–1132, 2020.

[41] A. F. Avila, M. O. dos Reis, S. G. Leão, and H. Nascimento, "Carbon nanotube reinforced epoxy based adhesive: correlations between chemical functional and failure modes," *International Journal of Adhesion and Adhesives*, vol. 119, 2022.

[42] F. Azimpour Shishevan, M. Mohtadi Bonab, and H. Akbulut, "The influence of addition of carbon nanotube and graphene platelets on characteristics of carbon/basalt fiber reinforced intra ply hybrid composites," *Journal of Applied Polymer Science*, vol. 140, 2023.

[43] I. Imoro, J. K. Nkrumah, B. Ziblim, and A. H. Mohammed, "Analysis of the material properties of vehicle suspension coil spring," *World Journal of Engineering and Technology*, vol. 11, pp. 827–858, 2023.

[44] A. S. Karad, P. D. Sonawwanay, and C. Y. Bachhav, "Finite element analysis of coil spring by using carbon fibre, carbon steel and epoxy resin materials," *Materials Today: Proceedings*, vol. 20, 2023.

[45] J. Ke, J. He, Z. Wu, and Z. Xiang, "Fatigue reliability design of composite helical spring with nonlinear stiffness based on ply scheme design," *Composite Structures*, vol. 319, 2023.

[46] C. Madrazo, *Carbon Fiber Coil Spring Characterization and Manufacturing*, University of Nevada, Las Vegas, Las Vegas, Nevada, 2022.

[47] M. Rahul and K. Rameshkumar, "Multi-objective optimization and numerical modelling of helical coil spring for automotive application," *Materials Today Proceedings*, vol. 46, pp. 4847–4853, 2021.

[48] A. R. Singh pankaj, W. Sanket, J. Viraj, and K. Patel, "Design and analysis of helical compression spring used in suspension system by finite element analysis method," *International Research Journal of Engineering and Technology (IRJET)*, vol. 4, 2017.

[49] S. Kumar, N. Rajesh, and P. Divakar, "Static analysis of a primary suspension spring used in locomotive," *International Journal of Mechanical Engineering and Robotics Research*, vol. 2, 2018.

[50] B. L. Choi and B. H. Choi, "Numerical method for optimizing design variables of carbon-fiber-reinforced epoxy composite coil springs," *Composites Part B: Engineering*, vol. 82, pp. 42–49, 2015/12/01/2015.

[51] P. P. K. Sagar N Khurd, "Probabilistic design of helical coil spring for longitudinal invariance by using finite element method," *Young*, vol. 3400, 2014.

[52] M. Bakhshesh and M. Bakhshesh, "Optimization of steel helical spring by composite spring," *International journal of multidisciplinary science and engineering*, vol. 3, 2012.

[53] D. A. Budan and T. Manjunatha, "Investigation on the feasibility of composite coil spring for automotive applications," *International Journal of Mechanical & Mechatronics Engineering*, vol. 4, pp. 1035–1039, 2010.

[54] M. Luger, R. Traxl, U. Hofer, B. Hirzinger, and R. Lackner, "RUC-based multi-scale model for braid-reinforced

polymers: application to coil springs," *Composites Part B: Engineering*, vol. 155, pp. 431–443, 2018/12/15/2018.

[55] V. R. Suresh and A. Thiagararajan, "Fabrication and analysis of nano composite cylindrical helical spring," *International Journal of Innovative Research in Science, Engineering and Technology*, vol. 3, 2014.

[56] S. G. Harale and M. Elango, "Design of helical coil suspension system by combination of conventional steel and composite material," *International Journal of Innovative Science Engineering and Technology (IJISET)*, vol. 3, pp. 15144–15150, 2014.

[57] H. B. Pawar, A. R. Patil, and S. B. Zope, "Design and analysis of a front suspension coil spring for three wheeler vehicle," *International Journal of Innovations In Engineering Research and Technology*, vol. 3, 2016.

[58] D. V. Shevale and N. D. Khaire, "Analysis of helical compression spring for estimation of fatigue life," *Imperial journal of interdisciplinary research*, vol. 2, 2016.

[59] C. K. Yogesh Chaubey, "Failure analysis of suspension coil spring for passenger car through SEM microstructure investigation," *International General of Innovation in Engineering and Technology (IGIET)*, vol. 25, 2016.

[60] P. J. Christopher and Pavendhan, *Design and Analysis of Two Wheeler Shock Absorber*, Coil Spring, Madhya Pradesh, India, 2014.

[61] S. Logavigneshwaran, G. Sriram, and R. Arunprakash, "Design and analysis of helical coil spring in suspension system," *International journal for trends in engineering & technology*, vol. 9, 2015.

[62] D. Pastorcic, G. Vukelic, and Z. Bozic, "Coil spring failure and fatigue analysis," *Engineering Failure Analysis*, vol. 99, pp. 310–318, 2019/05/01/2019.

[63] A. Nirala, N. Kumar, D. Bandhu Singh et al., "Simulation analysis of composite helical spring for compression, torsional and transverse mode," *Materials Today: Proceedings*, vol. 28, pp. 2263–2267, 2020/01/01/2020.

[64] A. Eatemadi, H. Daraee, H. Karimkhanloo et al., "Carbon nanotubes: properties, synthesis, purification, and medical applications," *Nanoscale Research Letters*, vol. 9, pp. 1–13, 2014.

[65] M. Berhane, *Weight Optimization of Front Coil Spring Suspension Using Composite Material for Bajaj by FEM*, Doctoral dissertation, AAU, Addis Ababa, Ethiopia, 2018.

[66] K. S. Pawar, A. K. Bagha, S. Bahl, and M. K. Agarwal, "Experimental investigation for the dynamic characteristics of short natural fiber reinforced composite materials," *Indian Journal of Engineering and Materials Sciences*, vol. 29, pp. 366–377, 2022.

[67] P. K. Mallick, *Fiber-reinforced Composites: Materials, Manufacturing, and Design*, CRC Press, Boca Raton, FL, USA, 2007.

[68] S. Km and N. Kundachira Subramani, "Fiber reinforced composites- a review," *Journal of Material Science & Engineering*, vol. 6, 01/01 2017.

[69] K. Varshney, "Carbon nanotube: a review on synthesis, properties and applications," *International Journal of Engineering Research*, vol. 2, pp. 07–26, 2014.

[70] Z. H. Jabbar, B. H. Graimed, A. A. Okab et al., "A review study summarizes the main characterization techniques of nanocomposite photocatalysts and their applications in photodegradation of organic pollutants," *Environmental Nanotechnology, Monitoring & Management*, vol. 19, 2023.

[71] S. A. Bansal, V. Khanna, A. P. Singh, and S. Kumar, "Small percentage reinforcement of carbon nanotubes (CNTs) in epoxy (bisphenol-A) for enhanced mechanical performance," *Materials Today: Proceedings*, vol. 61, pp. 275–279, 2022.

[72] M. Sudhakar Reddy and B. Madhusudhan Reddy, "The study of premature failure of springs used in railway coaches," *IOSR Journal of Mechanical and Civil Engineering*, vol. 8, pp. 19–28, 2013.

[73] P. B. Tapkir and B. Nelge, "Fatigue Life Prediction of Composite Semi-Elliptical Leaf Spring for Heavy Vehicle," *International Journal of Engineering Sciences & Research Technology*, vol. 4, no. 6, pp. 194–199, 2015.

[74] I. Elfaleh, F. Abbassi, M. Habibi et al., "A comprehensive review of natural fibers and their composites: an eco-friendly alternative to conventional materials," *Results in Engineering*, vol. 23, 2023.

[75] G. Dou, G. Peng, Y. Hu, Y. Sun, H. Jiang, and T. Zhang, "Effects of interface bonding on the macro-mechanical properties of microcapsule/epoxy resin composites," *Surfaces and Interfaces*, vol. 34, 2022.

[76] S. R. Mousavi, S. Estaji, H. Kiaei et al., "A review of electrical and thermal conductivities of epoxy resin systems reinforced with carbon nanotubes and graphene-ba/sed nanoparticles," *Polymer Testing*, vol. 112, 2022.

[77] A. Dweepan, "Innovative material selection and optimization of conventional springs," *International Journal Of Research In Aeronautical And Mechanical Engineering*, vol. 2, pp. 44–49, 2014.

[78] K. Hadgu, *Development of Composite Helical Coil Spring for Light Weight Vehicle*, Addis Ababa University, Addis Ababa, Ethiopia, 2013, https://etd.aau.edu.et/handle/123456789/23623.

[79] N. P. Singh, V. K. Gupta, and A. P. Singh, "Graphene and carbon nanotube reinforced epoxy nanocomposites: a review," *Polymer*, vol. 180, 2019.

[80] T. M. D Abdul Budan, "Carbon fiber reinforced composite coil springs," in *Proceedings of the International Conference on Advances in Industrial and Production Engineering*, pp. 17–21, Pittsburgh, PA, USA, June 2011.

[81] I. V. Andrianov, J. Awrejcewicz, and G. A. Starushenko, *Approximate Models of Mechanics of Composites: An Asymptotic Approach*, CRC Press, Boca Raton, FL, USA, 2023.

[82] A. K. C. P. Kaw, *Mechanics of Composite Materials*, Courier Corporation, Chelmsford, MA, USA, 2nd edition, 2005.

[83] J. Njuguna, K. Pielichowski, and J. R. Alcock, "Epoxy based fibre reinforced nanocomposites," *Advanced Engineering Materials*, vol. 9, pp. 835–847, 2007.

[84] J. Njuguna, K. Pielichowski, and J. Fan, "Polymer nanocomposites for aerospace applications," *Advances in Polymer Nanocomposites*, vol. 23, pp. 472–539, 2012.

[85] F. H. Gojny and K. Schulte, "Functionalisation effect on the thermo-mechanical behaviour of multi-wall carbon nanotube/epoxy-composites," *Composites Science and Technology*, vol. 64, pp. 2303–2308, 2004.

[86] R. G. de Villoria, A. Miravete, J. Cuartero, A. Chiminelli, and N. Tolosana, "Mechanical properties of SWNT/epoxy composites using two different curing cycles," *Composites Part B: Engineering*, vol. 37, pp. 273–277, 2006.

[87] K. T. Lau and S. Q. Shi, "Failure mechanisms of carbon nanotube/epoxy composites pretreated in different temperature environments," *Carbon*, vol. 40, p. 2965, 2002.
[88] M. K. Buragohain, *Composite Structures: Design, Mechanics, Analysis, Manufacturing, and Testing*, CRC Press, Boca Raton, FL, USA, 2017.
[89] E. Egorikhina, S. Bogovalov, and I. Tronin, "Determination of mechanical characteristics of unidirectional fiber composites," *Physics Procedia*, vol. 72, pp. 66–72, 2015.
[90] A. D. Anto, S. Mia, and M. A. Hasib, "The influence of number and orientation of ply on tensile properties of hybrid composites," *Journal of Physics: Materials*, vol. 2, 2019.
[91] S. C. Walpole, D. Prieto-Merino, P. Edwards, J. Cleland, G. Stevens, and I. Roberts, "The weight of nations: an estimation of adult human biomass," *BMC Public Health*, vol. 12, pp. 1–6, 2012.
[92] R. G. Budynas and J. K. Nisbett, *Shigley's Mechanical Engineering Design*, Mc Graw Hill, New York, NY, USA, 2015.
[93] J. Gupta and R. Khurmi, *A Textbook of Machine Design*, S. Chand Publications, New Delhi, India, 14th edition, 2005.
[94] J. Mandell, D. Huang, and F. McGarry, "Tensile fatigue performance of glass fiber dominated composites," *Journal of Composites Technology and Research*, vol. 3, pp. 96–102, 1981.
[95] R. Huston, "Fatigue life prediction in composites," *International Journal of Pressure Vessels and Piping*, vol. 59, pp. 131–140, 1994.
[96] T. Putra and Husaini, "Identifying strain signal characteristics of automotive suspension system subjected to road surface vibrations," *AIP Conference Proceedings*, vol. 1983, 2018.
[97] M. C. Choukimath, N. R. Banapurmath, F. Riaz et al., "Experimental and computational study of mechanical and thermal characteristics of h-BN and GNP infused polymer composites for elevated temperature applications," *Materials*, vol. 15, p. 5397, 2022.
[98] A. Y. Patil, C. Hegde, G. Savanur et al., "Biomimicking nature-inspired design structures—an experimental and simulation approach using additive manufacturing," *Biomimetics*, vol. 7, p. 186, 2022.
[99] H. B. Pawar and D. D. Desale, "Optimization of three wheeler front suspension coil spring," *Procedia Manufacturing*, vol. 20, pp. 428–433, 01/01 2018.